Canadian Journal of Research

Issued by THE NATIONAL RESEARCH COUNCIL OF CANADA

VOL. 28, SEC. F. AUGUST, 1950 NUMBER 8

HEAT TRANSFER IN A FLUIDIZED SOLIDS BED[1]

BY A. BAERG,[2] J. KLASSEN, AND P. E. GISHLER

Abstract

Heat transfer coefficients have been determined in a fluidized solids bed under a wide variety of conditions. The variables studied were particle size, bulk density under nonfluidized conditions, particle shape, and air velocity. Simple correlations have been established predicting the value of h in the air flow range investigated. An equation predicting the minimum fluidizing velocity has also been derived.

Introduction

The chemical industry today is finding that the solids fluidization technique can be applied with advantage to many diverse processes. This operation consists of bringing a bed of finely divided solids into a state of continuous agitation by passing a stream of gas or liquid upward through the particles.

This method of contacting fluids and solids has been employed for some considerable time. For example, in water treatment plants the supernatant layer of flocculating agent and sediment on the sand filters is removed by reversing the flow of water. The upward stream carries these materials to waste and serves to redistribute the sand particles.

It is only in recent years, however, that solids fluidization has come to be exploited as a chemical engineering tool. The chief application to date has been in the catalytic cracking of petroleum. Other uses, such as the calcining of limestone (1) and the roasting of sulphide concentrates (9), have been tested and applied.

Current interest is due to the superiority of this technique over other conventional types of unit processes, especially where the fluidized particles serve as a catalyst for reactions involving gases or vapors. Operations can be carried out continuously and so eliminate costly shutdown of equipment for the replacement or regeneration of the bed. Where surface phenomena are involved, the fine particles required for fluidization make available a larger surface which reduces the size of units required for a given throughput

[1] *Manuscript received March 3, 1950.*
Contribution from the Chemical Engineering Section, Division of Applied Chemistry, National Research Laboratories, Ottawa, Canada. Issued as N.R.C. No. 2178.
[2] *Present address—McGill University, Montreal, P.Q.*

of material. The bed is well suited for reactions in which the temperature is critical because the temperature gradient is very small.

It has been found possible to control temperatures by submerging heat exchangers in a fluidized solids bed. Heat transfer rates are many times those for a fixed bed and therefore, fluidizing is especially superior in carrying out reactions in which the heat involved is large. While numerous papers have appeared in the literature in the last few years (2, 3, 4, 7, 8, 12, 13) which deal with the hydraulics and mechanics of fluidized beds, it is only recently that work on heat transfer has been published. Mickley and Trilling (10) determined heat transfer coefficients in beds of glass beads of various sizes at linear gas velocities above 2 ft. per sec., while Leva, Weintraub, and Grummer (5) studied silica sands and iron catalysts. The range of sizes in this investigation was limited. The present paper deals with a variety of materials ranging in size from 20 to 325 mesh. Gas rates varied from below the minimum fluidizing velocity to rates at which the carry-over of solids in the gas stream was large.

The work consisted of determining heat transfer coefficients for heat flowing from a centrally located copper tube into a bed of fluidized particles. For the bulk of the work each bed contained a closely sized cut of one material. However, in order to determine the influence of wider size ranges, several runs were also made with mixtures of two different sizes.

Apparatus

The heat transfer unit is shown in Fig. 1. It consisted essentially of a heavy walled brass cylinder of 5.5 in. internal diameter and 22 in. high containing a solids bed approximately 10 in. deep. These dimensions were adopted in order to minimize such unfavorable phenomena as slugging, channeling, and segregation of sizes. The grid was a perforated plate covered with a 325 mesh copper screen.

The heat exchanger consisted of an electric cartridge heater supported inside a thick-walled copper tube of 1.25 in. outside diameter and 4 in. long. The space between the heater and the inside surface of the copper tube was filled with a low melting alloy (Wood's metal) that was fluid at the temperature of the experiment and therefore provided uniform lateral heat flow to the copper wall. The copper tube was centrally positioned by supports which were made of plastic in order to minimize thermal end losses. The lower support was a polystyrene rod which was machined to fit as indicated in detail in Fig. 1. A groove in this rod carried the leads for the thermocouples used to measure the temperature of the copper wall. The thermocouple leads terminated at recessed bands near the base of the polystyrene rod.

Thirty gauge copper–constantan thermocouples were embedded in holes of 0.0465 in. diameter in the copper tube, according to the method of Mohun and Peterson (11). This design made it possible to obtain accurate wall

temperatures without disturbing the flow of fluidized solids past the heater wall. E.m.f.'s were measured with a Rubicon potentiometer.

The upper heat exchanger support was a thick-walled bakelite tube of 1.25 in. outside diameter which was screw-fitted to the copper tube. This carried

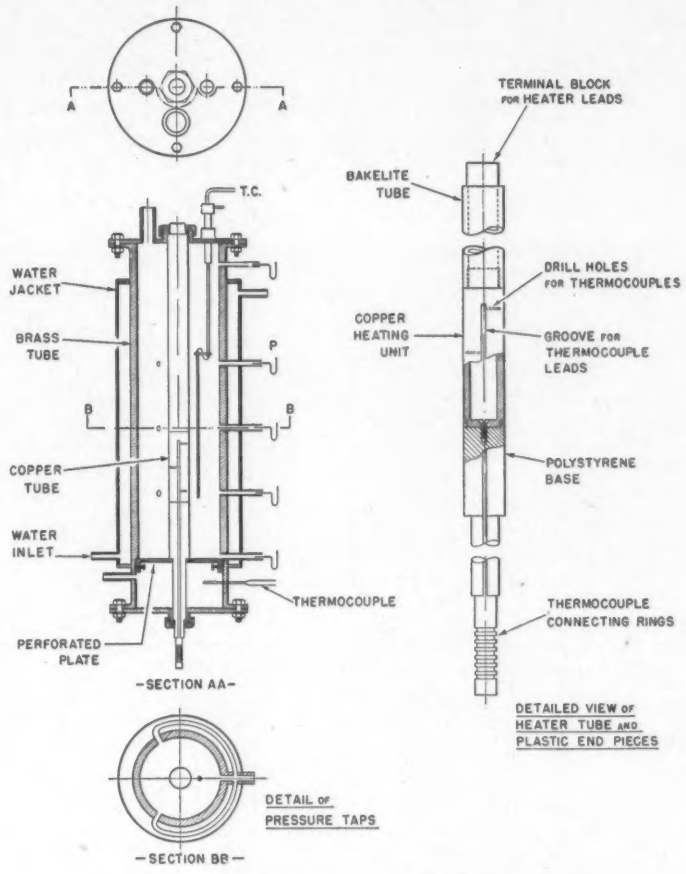

FIG. 1. *Heat transfer unit.*

the leads to the cartridge heater. Measurements of the power input to the heater were made with a calibrated voltmeter and ammeter for some of the tests. For the remainder a precision wattmeter was used.

The large brass cylinder containing the solids bed was water-jacketed. This served to maintain a high temperature differential between the heater and bed, and permitted rapid establishment of temperature equilibrium between the heat exchanger and the bed. Bed temperatures were obtained

by employing a thermocouple which could be moved vertically and also swiveled laterally. Nine bed temperatures were read for each determination of the heat transfer coefficient, three across the bed at the upper, middle, and lower levels of the copper tube.

The fluidizing gas used was air. The flow rate was measured by means of a rotameter. A glass cyclone separator removed solids entrained in the exit air stream and returned them to the bed through a standpipe, as illustrated in Fig. 2. Six manometers permitted the determination of pressure drops throughout the system. Each was connected to a piezometer ring, as shown in Fig. 1.

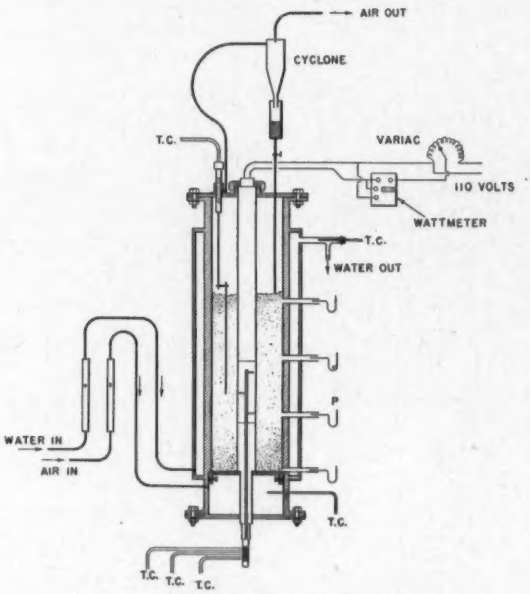

FIG. 2. *Diagrammatic sketch of apparatus.*

Experimental

The relevant properties of the materials included in this work are recorded in Table I. The particle diameter was determined microscopically; each value given is the average of 100 individual measurements.

Pycnometers were employed to obtain the absolute densities. The bulk densities were measured by pouring the material into a graduated cylinder and recording the volume and weight.

Heat transfer coefficients were measured in beds of materials of one particular size over a wide range of air flow rates. Determinations were first made at one or more air rates in the region below the minimum fluidizing

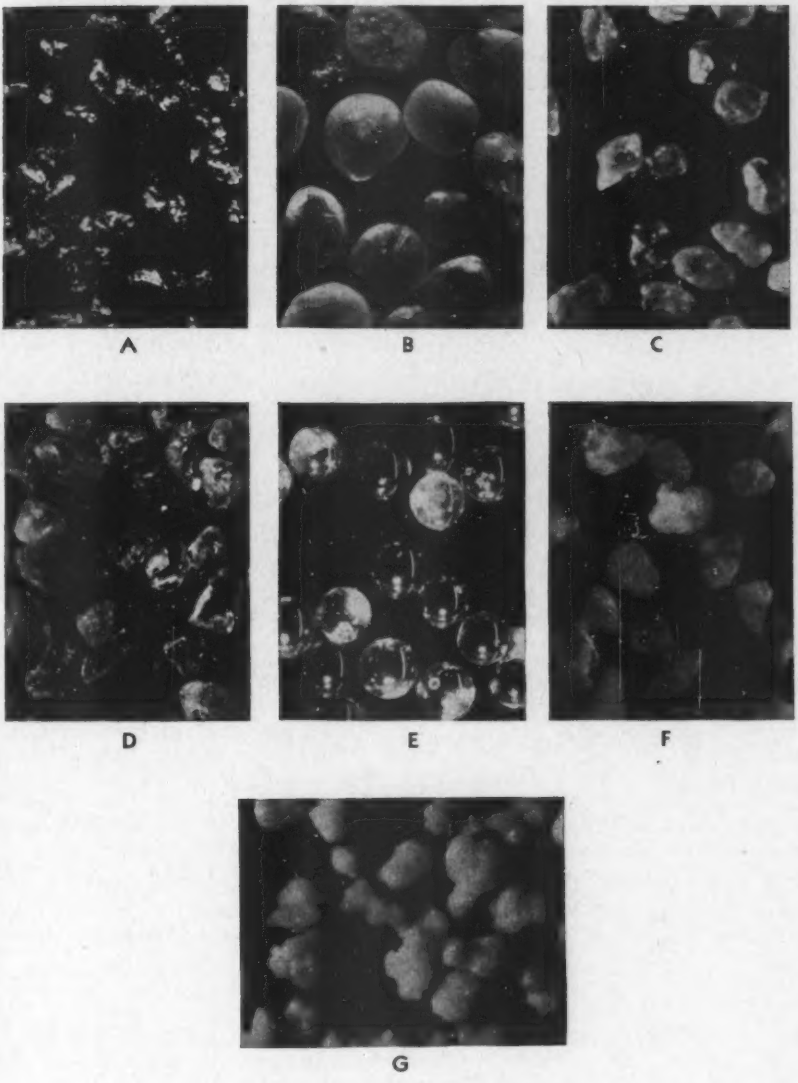

FIG. 3. *Photomicrographs of materials.*

	Material	*Dp, ft.*
A	*Iron powder*	*0.000986*
B	*Round sand*	*0.00288*
C	*Foundry sand*	*0.000714*
D	*Jagged silica*	*0.00165*
E	*Scotchlite beads*	*0.000519*
F	*Cracking catalyst*	*0.000457*
G	*Alumina*	*0.000385*

TABLE I

PHYSICAL PROPERTIES OF THE SOLID PARTICLES

Material	Particle diameter, ft.	Absolute density, lb./cu. ft.	Bulk density, lb./cu. ft.	Per cent voids
Iron powder	0.00123	423	148	65.0
Iron powder	0.000986	416	134	67.7
Iron powder	0.000640	434	135	69.0
Round sand	0.00288	145	89.0	38.8
Round sand	0.00106	146	81.7	44.0
Foundry sand	0.000905	143	82.9	42.0
Foundry sand	0.000714	142	82.5	42.0
Foundry sand	0.000525	140	79.7	43.0
Foundry sand	0.000419	140	74.4	47.0
Jagged silica	0.00242	147	76.3	48.0
Jagged silica	0.00165	142	70.8	50.0
Jagged silica	0.00103	139	68.9	50.5
Scotchlite beads No. 7	0.00151	176	104.2	40.9
Scotchlite beads No. 11	0.000519	153	89.2	41.7
Scotchlite beads No. 15	0.000198	148	84.3	42.7
Cracking catalyst	0.000457	124	31.0	75.0
Cracking catalyst	0.000320	119	32.6	72.5
Alumina	0.000385	167	64.0	61.7
Alumina	0.000312	165	65.1	60.5

velocity, and then at increasingly higher air rates until the air mass velocity G reached a value of approximately 400 lb./ (hr.) (sq. ft.).

Nineteen beds, as listed and described in Table I, were investigated. Fig. 3 shows photomicrographs of particles of each of the seven materials in order to indicate the shape of the particles.

In the nonfluidized bed there was a considerable temperature gradient across the bed. In the fluidized state this gradient was very low. At air

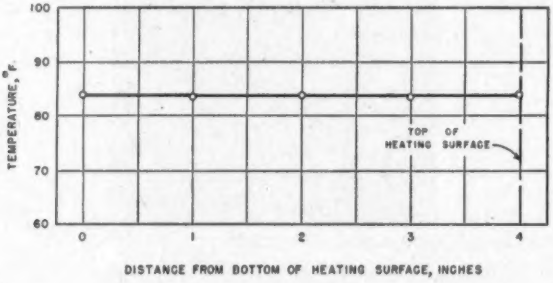

FIG. 4. *Typical longitudinal temperature profile of fluidized bed.*

velocities which caused only feeble agitation of the particles there was a vertical bed gradient near the heater wall with the temperatures near the base of the heater higher than at the top, indicating a co-ordinated downward flow of particles at the heater wall. For these conditions average temperatures were taken to calculate h. At high air rates the bed temperature

was uniform. This is illustrated in Figs. 4 and 5. From heat balance calculations for some of the runs it was found that only about 10% of the heat flowing from the heated copper surface to the fluidized bed left the system in the air passing out of the unit. The remaining 90% was removed by the water flowing in the outer jacket. This required a temperature difference of about 6°F. from the bed to the outer wall of the bed. As no thermocouples were embedded in this surface, accurate cold wall temperatures were not

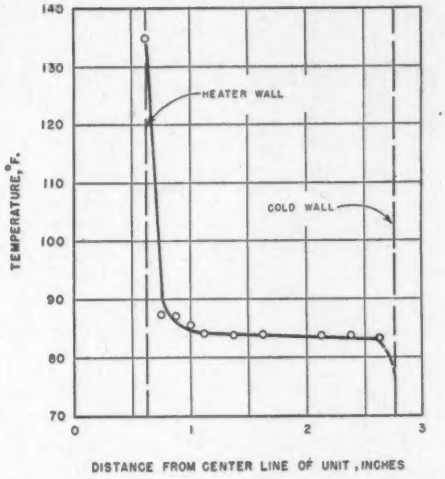

FIG. 5. *Typical radial temperature profile of fluidized bed.*

obtained. Therefore the radial temperature profile in Fig. 5 near the cold wall is shown in a broken line and depicts conditions as they must be to be consistent with the heat balance rather than conditions found by experimental temperature measurements. During an experiment the power input was adjusted to maintain a temperature difference of 40 to 50° F. between the copper wall and the bed. Beds were at approximately room temperature.

Results

Some preliminary runs were done with no solids in the unit. The air entered the heat transfer chamber through the perforations of the grid as a series of jets and was therefore in an extremely turbulent condition. This caused heat transfer coefficients between the wall and the air to be considerably higher than those predicted for the flow of air through a length of tube preceded by a calming section. The presence of a bed of solids would smother this jet effect a very short distance above the grid. It was considered that by locating the heated copper tube 2 in. above the grid, heat transfer would occur well within the region of normal fluidization. To test this, the apparatus was altered by placing the copper tube 4 in. above the grid. No significant

difference in heat transfer coefficients was detected, indicating that no irregular effects existed at the 2 in. level above the grid.

The unit was designed to hold a wide shallow bed to minimize slugging and to ensure smooth uniform fluidization. This is reflected in the data which in all tests fell on regular and continuous curves with but slight deviation.

The data for the 19 beds studied are given in Tables II to XX. The general shape of the heat transfer curve is indicated in Fig. 6, where h is

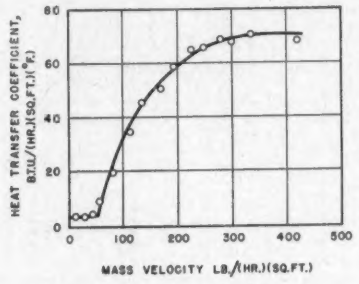

FIG. 6. *Typical heat transfer curve illustrated with data on round sand* (D_p = 0.00106 ft.).

plotted against G, the air mass velocity. At air rates below those required to fluidize the bed, the heat transfer coefficient was found to be low, being of the order of 4 B.t.u./ (hr.) (sq. ft.) (°F.) and increasing slightly with an increase in G.

The start of fluidization was indicated by a sharp discontinuous increase in the value of h. The mass velocity at which this discontinuity occurred is termed the minimum fluidizing velocity. As would be expected, G_{mf}

TABLE II

HEAT TRANSFER DATA

Iron powder. Diam. = 0.00123 ft.

U	G	T_w	T_b	ΔT	Q	h
0.21	56	142.3	78.2	64.1	271	4.23
0.41	112	137.4	78.2	59.2	294	4.97
0.52	141	136.0	75.9	60.1	294	4.90
0.55	149	126.3	76.9	49.4	292	5.9
0.57	155	132.9	79.9	53.0	1402	26.5
0.61	165	119.7	80.4	39.3	1669	42.5
0.73	197	117.9	81.2	36.7	1940	52.9
0.83	225	119.2	80.4	38.8	2277	58.6
0.94	253	115.4	79.7	35.7	2280	63.9
1.05	283	112.1	79.0	33.1	2256	68.2
1.25	339	111.4	79.3	32.1	2272	70.8
1.42	385	107.0	76.2	30.8	2273	73.8
1.47	398	110.7	79.6	31.1	2298	73.8
1.59	430	107.3	75.7	31.6	2275	72.0

TABLE III

HEAT TRANSFER DATA

Iron powder. Diam. = 0.000986 ft.

U	G	T_w	T_b	ΔT	Q	h
0.10	28	136.6	76.3	60.3	208	3.45
0.21	56	138.4	75.8	62.6	255	4.1
0.31	84	125.8	81.1	44.7	802	17.9
0.41	112	126.9	78.9	48.0	1657	34.5
0.52	140	121.9	78.1	43.8	2017	46.0
0.62	169	116.8	77.6	39.2	2258	57.6
0.73	196	110.0	74.2	35.8	2273	63.5
0.83	225	106.0	73.5	32.5	2268	69.8
0.94	253	103.7	73.4	30.3	2273	75.0
1.15	310	101.5	73.1	28.4	2273	80.1
1.36	368	100.1	72.9	27.2	2247	82.6
1.58	426	101.2	73.0	28.2	2273	81.0

TABLE IV

HEAT TRANSFER DATA

Iron powder. Diam. = 0.000640 ft.

U	G	T_w	T_b	ΔT	Q	h
0.053	14.4	130.3	75.0	55.3	187	3.4
0.107	29	134.7	74.9	59.8	209	3.5
0.16	43	139.6	74.2	65.4	225	3.4
0.21	56	128.7	73.5	55.2	868	15.7
0.31	84	114.7	75.0	39.7	1362	34.3
0.42	113	113.7	74.7	39.0	1939	49.7
0.52	141	111.6	74.3	37.3	2290	61.4
0.73	197	103.9	72.8	31.1	2287	73.5
0.94	254	101.1	72.0	29.1	2292	78.8
1.15	312	99.4	71.9	27.5	2311	84.1
1.37	370	98.3	71.5	26.8	2311	86.2
1.58	428	97.7	71.4	26.3	2311	87.9

TABLE V

HEAT TRANSFER DATA

Round sand. Diam. = 0.00288 ft.

U	G	T_w	T_b	ΔT	Q	h
0.285	77	120.8	79.9	40.9	209	5.11
0.48	130	117.0	80.6	36.4	209	5.74
0.67	182	137.4	83.4	54.0	367	6.80
0.87	235	136.6	80.6	56.0	704	12.55
1.08	292	128.8	80.6	48.2	1374	28.5
1.29	350	129.2	80.8	48.4	1905	39.4
1.50	407	130.9	81.0	49.9	2240	44.9
1.75	472	129.1	80.3	48.8	2240	45.9
1.99	537	128.9	79.6	49.3	2240	45.4
2.24	605	129.1	79.0	50.1	2240	44.7

TABLE VI

HEAT TRANSFER DATA

Round sand. Diam. = 0.00106 ft.

U	G	T_w	T_b	$\triangle T$	Q	h
0.054	14.7	139.5	82.1	57.4	218	3.8
0.11	29	132.3	78.4	53.9	209	3.9
0.16	44	136.2	77.9	58.3	259	4.4
0.21	56	132.2	74.5	57.7	536	9.3
0.31	83	127.1	75.7	51.4	1135	19.7
0.42	113	136.9	77.4	59.5	2034	34.2
0.50	136	127.0	76.9	50.1	2255	45.1
0.63	170	121.3	75.5	45.8	2315	50.6
0.72	195	114.0	75.5	38.5	2269	58.9
0.84	227	110.6	74.5	36.1	2333	64.6
0.93	250	111.2	76.7	34.5	2273	65.8
1.04	282	109.4	75.9	33.5	2301	68.7
1.11	300	109.3	76.1	33.2	2245	67.8
1.24	338	108.2	75.7	32.5	2280	70.2
1.56	422	107.8	74.5	33.3	2269	68.2

TABLE VII

HEAT TRANSFER DATA

Foundry sand. Diam. = 0.000905 ft.

U	G	T_w	T_b	$\triangle T$	Q	h
0.051	13.9	139.0	83.0	56.0	213	3.81
0.11	29.8	137.1	84.5	52.6	213	4.06
0.30	81.1	128.0	73.1	54.7	1582	28.9
0.72	195	113.3	73.2	40.1	2495	62.2
0.51	139	116.1	73.8	42.3	2168	51.3
0.98	264	110.0	74.3	35.7	2495	69.9
1.21	327	109.1	74.4	34.7	2495	71.9
1.44	390	114.9	74.3	40.6	2838	69.9
1.72	465	115.1	74.7	40.4	2838	70.3

TABLE VIII

HEAT TRANSFER DATA

Foundry sand. Diam. = 0.000714 ft.

U	G	T_w	T_b	$\triangle T$	Q	h
0.051	13.9	141.9	85.5	56.4	213	3.79
0.104	28.0	107.9	75.5	32.4	218	6.74
0.31	84.6	124.2	75.7	48.5	1725	35.6
0.53	142	121.6	75.7	43.9	2495	56.8
0.74	200	119.8	75.2	44.6	2825	63.4
0.98	264	114.3	74.9	39.4	2825	71.7
1.20	325	110.8	73.5	37.3	2825	75.8
1.46	394	109.4	73.5	35.9	2825	78.7
1.72	464	110.1	73.2	36.9	2825	76.6

TABLE IX

HEAT TRANSFER DATA

Foundry sand. Diam. = 0.000525 ft.

U	G	T_w	T_b	$\triangle T$	Q	h
0.051	13.9	142.2	84.7	57.5	213	3.71
0.162	44.0	133.4	74.8	58.6	1115	19.0
0.26	71.0	133.5	77.4	56.1	2200	39.2
0.58	156	118.5	77.0	41.5	2850	68.7
0.87	236	111.6	75.3	36.3	2825	77.8
1.08	292	109.2	75.9	33.3	2825	84.8
1.30	350	108.5	75.3	33.2	2825	85.9
1.51	408	109.6	75.7	33.9	2835	83.7
1.75	473	109.7	75.7	34.0	2835	83.4
1.99	537	109.7	75.4	34.3	2835	82.8
2.24	605	109.5	75.3	34.2	2835	82.9

TABLE X

HEAT TRANSFER DATA

Foundry sand. Diam. = 0.000419 ft.

U	G	T_w	T_b	$\triangle T$	Q	h
0.015	4.2	126.9	83.1	43.8	192	4.39
0.043	11.0	143.7	87.1	56.6	380	6.71
0.118	32	131.5	76.4	55.1	112	20.3
0.28	77	130.5	79.5	51.0	2580	50.6
0.48	130	123.6	78.2	45.4	2925	64.4
0.67	182	116.2	76.5	39.7	2925	73.7
0.87	235	111.8	75.8	36.0	2925	81.2
1.08	292	108.3	75.5	32.8	2925	89.2
1.30	350	107.9	75.1	32.8	2925	89.2
1.51	407	107.8	75.2	32.6	2925	89.7
1.75	472	107.8	74.9	32.9	2925	88.9
1.99	537	107.7	74.9	32.8	2925	89.2
2.24	605	107.9	74.7	33.2	2925	88.1

TABLE XI

HEAT TRANSFER DATA

Jagged silica. Diam. = 0.00242 ft.

U	G	T_w	T_b	$\triangle T$	Q	h
0.52	140	127.4	62.7	64.7	366	5.66
0.73	198	131.9	66.7	65.2	443	6.80
0.84	226	128.4	67.2	61.2	1229	20.0
0.94	255	122.8	68.5	54.3	1664	30.3
1.05	284	121.9	68.6	53.3	1971	37.0
1.16	313	122.1	68.8	53.3	2251	42.2
1.25	339	121.1	69.2	51.9	2389	46.1
1.36	368	118.0	68.8	49.2	2389	48.6
1.47	398	116.5	68.5	48.0	2389	49.8
1.58	426	115.2	68.2	47.0	2389	50.8
1.69	456	115.9	68.3	47.6	2389	50.2

TABLE XII

HEAT TRANSFER DATA

Jagged silica. Diam. = 0.00165 ft.

U	G	T_w	T_b	ΔT	Q	h
0.21	56	117.1	68.0	49.1	207	4.2
0.31	84	118.5	68.4	50.1	224	4.5
0.41	112	121.8	74.7	47.1	834	17.7
0.52	141	116.1	70.9	45.2	1707	37.7
0.62	169	113.5	69.4	44.1	1990	45.1
0.73	197	117.7	69.0	48.7	2420	49.8
0.83	225	113.7	68.0	45.7	2422	53.0
0.93	251	109.3	67.6	41.7	2370	56.8
1.04	282	107.4	67.1	40.3	2370	58.7
1.26	340	106.5	67.1	39.4	2370	60.1
1.47	398	106.9	66.7	40.2	2430	60.3
1.69	457	108.7	68.7	40.0	2400	60.0

TABLE XIII

HEAT TRANSFER DATA

Jagged silica. Diam. = 0.00103 ft.

U	G	T_w	T_b	ΔT	Q	h
0.118	32	137.0	82.6	54.4	210	3.86
0.285	77	127.6	78.0	49.6	1360	27.5
0.481	130	130.9	79.9	51.0	2358	46.2
0.684	185	126.5	79.3	47.2	2925	62.0
0.877	235	121.5	78.5	43.0	2925	68.1
1.08	292	119.8	78.3	41.5	2925	70.5
1.29	350	119.5	78.4	41.1	2925	71.2
1.51	407	119.2	79.5	41.7	2925	70.2
1.75	472	119.5	78.1	41.4	2925	70.7
1.99	537	119.3	77.8	41.5	2925	70.5

TABLE XIV

HEAT TRANSFER DATA

Scotchlite beads, No. 7. Diam. = 0.00151 ft.

U	G	T_w	T_b	ΔT	Q	h
0.0825	22	135.5	81.2	54.3	196	3.62
0.120	32	146.3	80.5	65.8	266	4.04
0.216	58	134.2	76.7	57.5	253	4.40
0.360	97	137.0	75.0	62.0	310	5.00
0.483	130	133.4	75.9	57.5	326	5.70
0.672	182	131.3	72.8	58.4	1320	22.6
0.880	235	127.9	79.9	48.0	2772	57.8
1.09	291	134.3	81.1	53.2	3823	71.9
1.27	340	129.0	80.1	48.9	3798	77.7
1.52	407	128.9	78.6	50.3	3798	75.5
1.75	470	125.0	75.3	49.7	3785	76.2

TABLE XV

HEAT TRANSFER DATA

Scotchlite beads, No. 11. Diam. = 0.000519 ft.

U	G	T_w	T_b	ΔT	Q	h
0.0837	22.0	130.9	88.8	42.1	141	3.50
0.122	32.0	122.2	89.2	33.0	791	24.0
0.153	41.6	121.2	70.5	50.7	1741	41.6
0.217	58.0	120.6	81.1	39.5	2545	64.4
0.417	111	121.6	81.3	40.3	2962	73.5
0.582	156	120.2	78.6	41.6	3646	87.6
0.777	208	117.7	79.1	38.6	3836	99.4
0.998	267	115.8	79.2	36.6	3836	104.8
1.20	320	116.6	79.5	37.1	3811	102.7
1.45	387	118.4	80.5	37.9	3912	103.3

TABLE XVI

HEAT TRANSFER DATA

Scotchlite beads, No. 15. Diam. = 0.000198 ft.

U	G	T_w	T_b	ΔT	Q	h
0.00740	1.95	130.5	86.9	43.6	120	2.76
0.045	12.0	126.4	79.8	46.6	589	12.6
0.120	32.0	127.2	79.8	47.4	2241	47.3
0.146	39.0	133.6	80.0	53.6	2785	52.0
0.186	49.8	133.4	79.5	53.9	2874	53.4
0.493	132	116.6	79.5	37.1	3912	105.3
0.642	172	112.5	78.7	33.8	3937	116.5
0.885	237	110.4	78.6	31.8	3963	124.6
1.08	290	109.5	78.3	31.2	3975	127.4
1.31	352	108.2	77.8	30.4	3975	130.4

TABLE XVII

HEAT TRANSFER DATA

Cracking catalyst. Diam. = 0.000457 ft.

U	G	T_w	T_b	ΔT	Q	h
0.0246	6.6	126.4	76.7	49.7	82	1.65
0.0433	11.7	130.5	73.9	56.6	475	8.38
0.0813	22.0	120.1	72.8	47.3	665	14.1
0.118	32.2	123.8	68.1	55.7	1263	22.7
0.155	42.1	122.5	70.7	51.8	1981	38.3
0.234	63.5	119.0	71.1	47.9	1978	41.4
0.333	90	122.3	74.6	47.7	2329	48.9
0.529	143	122.5	74.1	48.4	3000	62.0
0.734	198	128.9	75.0	53.8	3608	67.1
0.927	250	128.2	75.2	53.0	3621	68.3
1.13	307	131.9	73.0	58.9	3912	66.5
1.34	365	128.8	71.6	57.2	3899	68.2

TABLE XVIII

HEAT TRANSFER DATA

Cracking catalyst. Diam. = 0.000320 ft.

U	G	T_w	T_b	$\triangle T$	Q	h
0.00703	1.85	144.8	87.9	56.9	111	1.95
0.0238	6.35	133.3	80.4	52.9	222	4.19
0.0446	12.0	123.7	75.7	48.0	479	9.96
0.0812	21.8	129.7	77.3	53.8	931	17.3
0.120	32.2	130.7	76.1	54.6	1158	21.2
0.176	47.3	122.5	75.9	45.2	1927	42.6
0.235	63.2	123.3	76.0	47.3	2278	48.2
0.339	91	123.8	78.4	45.4	2709	59.7
0.533	143	122.6	78.4	44.2	3152	71.3
0.728	195	121.3	78.6	42.7	3140	73.4
0.932	250	121.3	78.3	43.0	3266	76.0
1.13	302	120.3	78.2	41.1	3228	76.7

TABLE XIX

HEAT TRANSFER DATA

Alumina. Diam. = 0.000385 ft.

U	G	T_w	T_b	$\triangle T$	Q	h
0.0575	15.5	132.0	75.6	56.4	623	11.1
0.0804	21.7	121.2	74.5	56.7	823	17.6
0.116	31.5	123.6	70.1	23.5	1257	23.5
0.156	41.8	123.2	77.8	45.4	1823	40.1
0.210	57.0	121.9	73.2	48.7	2228	45.7
0.278	76.0	118.1	68.2	49.9	3013	60.4
0.584	158	117.8	73.5	44.3	3241	73.2
0.780	210	122.0	75.7	46.3	3823	82.5
1.01	272	123.3	78.6	44.7	3874	86.6
1.22	325	125.7	79.8	45.9	3950	86.0
1.39	382	109.3	63.3	46.0	3811	82.8
1.59	437	109.3	63.6	45.7	3836	83.8

TABLE XX

HEAT TRANSFER DATA

Alumina. Diam. = 0.000312 ft.

U	G	T_w	T_b	$\triangle T$	Q	h
0.0571	15.5	110.7	72.0	38.7	636	16.4
0.0821	22.5	103.6	66.8	36.8	1222	33.2
0.117	32.0	100.8	66.2	34.6	1488	43.1
0.154	42.2	108.9	67.4	41.5	2184	52.6
0.212	58.5	112.2	63.8	48.4	3070	63.4
0.510	140	109.1	65.4	43.7	3228	73.9
0.658	180	102.7	67.3	35.4	3165	89.3
0.778	212	110.0	69.8	40.2	3925	97.5
0.967	265	106.9	67.0	39.9	3766	94.4
1.18	322	107.4	67.4	40.0	3823	95.5

varies in a direction proportional to the particle diameter and bulk density. The data cover a tenfold variation in particle diameter, a threefold variation in bulk density and widely different particle shapes. The experimental results are contained in Table XXI. An increase in G above G_{mf} resulted in an initial rapid rise in h, followed by a more gradual rate of increase until

TABLE XXI

FLUIDIZATION AND HEAT TRANSFER CHARACTERISTICS

Material	D_p	G_{mf}	h_{max}
Iron powder	0.00123	145	73.8
Iron powder	0.000986	70	82.6
Iron powder	0.000640	45	87.9
Round sand	0.00288	211	45.9
Round sand	0.00106	42	70.2
Foundry sand	0.000905	46	71.9
Foundry sand	0.000714	30	78.7
Foundry sand	0.000525	22	85.9
Foundry sand	0.000419	10	89.7
Jagged silica	0.00242	196	50.8
Jagged silica	0.00165	85	60.3
Jagged silica	0.00103	44	71.2
Scotchlite beads, No. 7	0.00151	130	77.7
Scotchlite beads, No. 11	0.000519	20	104.8
Scotchlite beads, No. 15	0.000198	5	130.4
Cracking catalyst	0.000457	10	68.3
Cracking catalyst	0.000320	5	76.7
Alumina	0.000385	15	86.6
Alumina	0.000312	11	97.5

a maximum value for h was reached. This maximum extended over a considerable range of G with evidence of a slight falling-off at the highest air rates studied. Heat transfer coefficient curves were established for several sizes of each material. It was found that the value of h_{max} increased with a decrease in particle size.

The data permitted the establishment of simple correlations which predicted the following:

1. The onset of fluidization.
2. The value of h_{max}.
3. The value of h at fluidizing rates below those required to yield h_{max}.

Discussion

1. The Onset of Fluidization

The determination of the minimum fluidizing velocity has been carried out experimentally by a number of workers by studying pressure drops across the bed. When the latter quantity is plotted against the gas flow rate there is a continuous increase until the initial fluidization point is reached. Here a sharp break in the curve occurs, and as higher gas velocities are attained the

pressure differential remains essentially constant. The discontinuity represents the minimum fluidizing mass velocity, G_{mf}. Wilhelm and Kwauk (13) and Leva *et al.* (2) have developed correlations from which G_{mf} can be predicted.

In the present work the minimum fluidizing mass velocity is taken as occurring at the discontinuity in the heat transfer curve. The values for the different materials are presented in Table XXI. The data are correlated by

$$G_{mf} = 1.3 \times 10^3 \, (D_p \rho_B)^{1.23*} \tag{1}$$

The curve for this equation along with the experimental points is shown in Fig. 7. Since the materials represent a wide variety of shapes, it must be

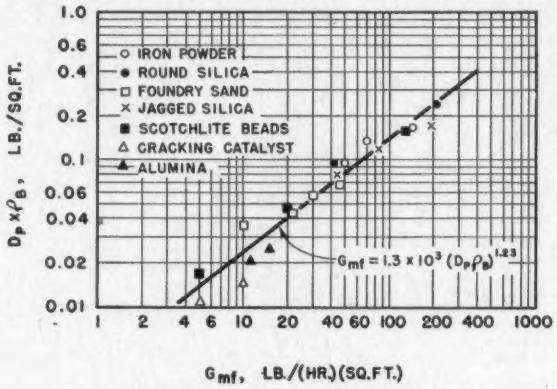

FIG. 7. *Correlation of minimum fluidizing velocity.*

concluded that shape plays only a minor role in determining G_{mf} except in its effect on the bulk density. Equation (1) results in a relatively simple and convenient method of predicting the point of initial fluidization, and requires only a minimum of material properties, all of which are readily measurable.

2. The Value of h_{max}

It was stated previously that the heat transfer coefficient for fluidized beds reached a maximum and remained at this value over a considerable air flow range. The plateau representing the maximum extended in most cases over the range of air velocities which is of most practical interest in the applied field of fluidized solids technique. It was therefore important to find a correlation relating h_{max} with the physical properties of the materials.

The values of h_{max} are listed in Table XXI. A satisfactory correlation results if D_p/ρ_B is plotted as abscissa on a logarithmic scale against h_{max} as

**The symbols in this and subsequent equations are defined near the end of the paper under the heading of notation.*

ordinate on a linear scale as in Fig. 8. The equation representing the data was found to be

$$h_{max} = 49 \log \left(\frac{0.00037}{D_p} \rho_B \right). \quad (2)$$

Some work on mixtures of foundry sands of two different sizes indicated that by using the average diameter and bulk density in Equation (2) the h_{max} which was found experimentally was predicted. Materials of different diam-

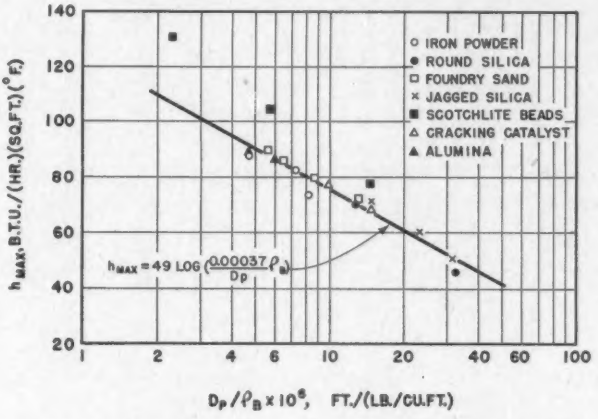

FIG. 8. *Correlation of maximum heat transfer coefficient.*

eters, densities, and shapes behaved according to the above expression. The data on Scotchlite glass beads, however, were an exception. The values for h_{max} determined experimentally were about 18% above those calculated by Equation (2). Under the microscope the beads appeared to be perfect spheres with an extremely smooth and polished surface. Particle shape could not account for the difference since all the other materials, which included particles of widely varying shapes, were correlated by Equation (2). The only apparent difference between the Scotchlite beads and the other materials was the almost complete absence of friction. The beads when rubbed between the fingers felt like a lubricant with very little frictional drag. It is possible that in a fluidized bed this would result in a freer movement with no effective intermeshing of particles and consequently in a higher value for h_{max}.*

Levenspiel and Walton (6) did work on heat transfer to beds of fluidized Utah coal and obtained curves similar in shape to those found here. They measured values of h which also reached a maximum at an air mass velocity

* *Work subsequent to the preparation of this paper indicated that the value of h_{max} for the Scotchlite beads is definitely affected by the surface roughness. The beads were etched with moist hydrogen fluoride gas and the surface, as viewed through a microscope, was roughened. The value of h_{max} of the etched material was substantially lower. Etching, however, had no effect on G_{mf}. Studies of this phase of the problem are continuing.*

of about 400 lb./ (hr.) (sq. ft.). The magnitude of the maximum they found, however, was considerably lower (i.e., of the order of 20 B.t.u./ (hr.) (sq. ft.) (° F)). It was suggested in the paper that coefficients considerably higher would result if more dense solids were employed.

Mickley and Trilling (10) have obtained data on glass beads at mass flow rates above those described in this paper. Their bed was much deeper and narrower and this, coupled with the higher flow rates, resulted in bed bulk densities considerably lower than those discussed here, with subsequently lower values of h. Leva *et al.* (5) measured heat transfer rates which are considerably lower than those reported here. In their case, heat transfer coefficients were measured for the outer heated wall. A study of the fluidization process in a glass unit reveals the fact that the movement of particles at the wall is considerably less vigorous than in the center of the bed. The present work

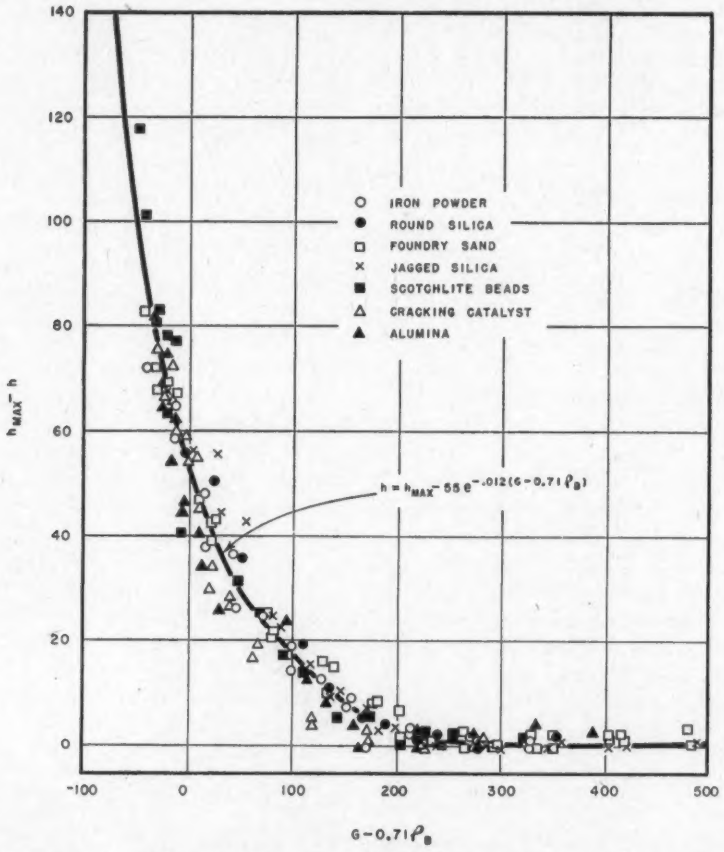

FIG. 9. *General correlation of heat transfer coefficients of all materials at varying mass velocities.*

was done with a small heat transfer surface in the center of a large fluidized bed and therefore the data do not apply to heat transfer through an outer surface. The two sets of results are therefore not on a comparable basis.

3. Intermediate Values of h

While the previous section correlates heat transfer coefficients over a considerable range of mass velocity, it does not include values of h at air rates below those required to yield h_{max}. The most successful correlation for these intermediate heat transfer coefficients results from the assumption that they approach h_{max} exponentially. This leads to the general expression

$$h - h_{max} = ae^{-bG}. \tag{3}$$

It was found, however, that while this type of equation had the same shape as all the experimental curves, there was a lateral displacement of the points from the mathematical curve along the abscissa or G axis. It was determined that this deviation was proportional to the bulk density of the particular material considered. When this fact is included in the relationship the equation assumes the form

$$h_{max} - h = ae^{-b(G-d\rho_B)}. \tag{4}$$

An evaluation of the constants by the application of standard graphical methods to the experimental data yields

$$h = h_{max} - 55e^{-0.012\,(G-0.71\rho_B)}. \tag{5}$$

All the measured values when plotted as $h_{max}-h$ against $G - 0.71\rho_B$ should fall on one curve. The plot has been made in Fig. 9 where the curve shown represents Equation (5). Typical data for one material of various particle diameters along with Equation (5) for each size can be seen in Fig. 10. All

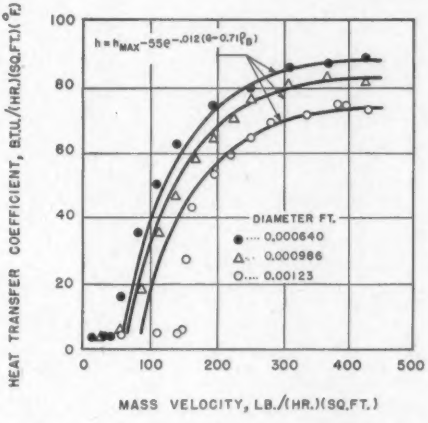

FIG. 10. *Heat transfer data and experimental equation for iron powders.*

of the particles studied except those of large diameter (i.e., $D_p > 0.0011$ ft.) have been found to apply. The deviations from Equation (5) increased rapidly as the diameter of the particles increased above 0.0011 ft.

Conclusions

1. A simple convenient formula for predicting the air velocity necessary to initiate fluidization has been derived. It is

$$G_{mf} = 1.3 \times 10^3 (D_p \rho_B)^{1.23}.$$

2. Maximum heat transfer coefficients for fluidized solids beds have been found to be mainly dependent on particle size and bulk density in the nonfluidized state. The equation

$$h_{max} = 49 \log \frac{0.00037}{D_p} \rho_B$$

successfully correlates the data for a wide variety of materials and sizes.

3. Heat transfer coefficients at air velocities below those required to yield h_{max} have been correlated by the following expression:

$$h = h_{max} - 55e^{-0.012(G-0.71\rho_B)}.$$

4. Limited work on mixtures of materials of two different sizes indicated that the above relationships are applicable if average particle diameters and bulk densities are used in the calculations.

5. It would appear that the value of the heat transfer coefficient is affected to very little extent by such factors as specific heat or specific conductivity.

6. This investigation gives no information on the effect of such variables as bed temperature, bed dimensions, and properties of the fluidizing gas.

Acknowledgments

The authors wish to thank Dr. Maurice Haycock for preparing the photomicrographs and Mr. W. S. Peterson for installing the thermocouples in the heater unit. Acknowledgment is made of the assistance of the Mines Branch, Ottawa, in supplying some of the sands used in this work.

Notation

a, b, d = experimental constants
e = base of natural logarithms = 2.718 . . .
D_p = particle diameter, ft.
G = mass velocity, lb./ (hr.) (sq. ft.)
G_{mf} = minimum fluidizing mass velocity, lb./ (hr.) (sq. ft.)
h = heat transfer coefficient, B.t.u./ (hr.) (sq. ft.) (° F.)
h_{max} = maximum heat transfer coefficient, B.t.u./ (hr.) (sq. ft.) (° F.)
Q = heat flux, B.t.u./ (hr.) (sq. ft.).

ρ_B = bulk density in the nonfluidized state, lb./cu. ft.
T_b = mean bed temperature, ° F.
T_w = wall temperature, ° F.
$\Delta T = T_w - T_b$, ° F.
U = linear air velocity based on the empty unit, ft./sec.

References

1. KITE, R. P. and ROBERTS, E. J. Chem. Eng. 54(12) : 112. 1947.
2. LEVA, M., GRUMMER, M., WEINTRAUB, M., and POLLCHIK, M. Chem. Eng. Progress, 44 : 511. 1948.
3. LEVA, M., GRUMMER, M., WEINTRAUB, M., and POLLCHIK, M. Chem. Eng. Progress, 44 : 619. 1948.
4. LEVA, M., GRUMMER, M., WEINTRAUB, M., and STORCH, H. H. Chem. Eng. Progress, 44 : 707. 1948.
5. LEVA, M., WEINTRAUB, M., and GRUMMER, M. Chem. Eng. Progress, 45 : 563. 1949.
6. LEVENSPIEL, O. and WALTON, J. S. Heat transfer and fluid mechanics institute, p. 139. Am. Soc. Mech. Engrs. New York. 1949.
7. LEWIS, W. K., GILLILAND, E. R., and BAUER, W. C. Ind. Eng. Chem. 41 : 1104. 1949.
8. MATHESON, G. L., HERBST, W. A., and HOLT, P. H., 2nd. Ind. Eng. Chem. 41 : 1099. 1949.
9. MATHEWS, O. Can. Mining Met. Bull. 42 : 178. 1949.
10. MICKLEY, H. S. and TRILLING, C. A. Ind. Eng. Chem. 41 : 1135. 1949.
11. MOHUN, W. H. and PETERSON, W. S. Can. Chem. Process Ind. 32 : 908. 1947.
12. MORSE, R. D. Ind. Eng. Chem. 41 : 1117. 1949.
13. WILHELM, R. H. and KWAUK, M. Chem. Eng. Progress, 44 : 201. 1948.

THE OXIDATION, DECOMPOSITION, IGNITION, AND DETONATION OF FUEL VAPORS AND GASES

XVI. BENZENE AS A KNOCKING FUEL IN CONDITIONS PROMOTING THE FORMATION OF FINELY DIVIDED CARBON[1]

By R. O. King,[2] E. J. Durand,[3] and A. B. Allan[4]

Abstract

Experiments are described which demonstrate that benzene becomes a knocking fuel when used in a spark ignition Otto cycle engine if operating conditions are such that the vapor–air mixture becomes impregnated with finely divided carbon. The carbon was obtained on the impingement of the flame of burning benzene on relatively cool surfaces in the combustion chamber and by the burning of liquid drops dispersed in a combustible vapor–air mixture. The droplets were obtained by wet carburation even when the over-all mixture was weak; the engine being run with low temperature coolant, low temperature air supply, and with the carburetor attached directly to the engine head.

Introduction

The effect of dispersions of finely divided material, even water, to ignite mixtures with air of combustible gases or vapors was described some years ago (6, 7). A theory of nuclear ignition based on the igniting effect of finely divided carbon was described accordingly in Part IV (1) to provide a working hypothesis for a systematic investigation of the detonation which limits the power and economy of Otto cycle spark ignition engines. The investigation has dealt with several aspects of the nuclear theory, and the experimental results have been given in Parts V to XV of a continuing series of papers published in Section F, Canadian Journal of Research.

Knocking combustion as distinct from detonation can be due to ignition of the gaseous mixture by overheated surfaces in the combustion chamber; this effect will be described as surface ignition. Surface ignition may occur prior to spark ignition and is then easily recognized and commonly described as preignition. It may also occur after spark ignition, and the consequent knocking combustion is, in many cases, difficult to distinguish from that due to detonation, especially as the effects may occur simultaneously, Part X (2).

Hydrogen, which cannot be decomposed to carbon, failed to detonate at a compression ratio of 10 : 1 until finely divided carbon was provided in sufficient concentration by pyrolysis of the lubricating oil or added to the entering air, Part V (10).

[1] *Manuscript received May 8, 1950.*
Contribution from Defence Research Board, Ottawa, Canada, in association with the Department of Mechanical Engineering, University of Toronto, Toronto, Ont.
[2] *Research Scientist, Defence Research Board, Ottawa.*
[3] *Lecturer, Mechanical Engineering, University of Toronto.*
[4] *Research Assistant, Mechanical Engineering, University of Toronto.*

Toronto town gas contains hydrocarbons in small proportion, approximately 15 to 20% including the methane. It is therefore not a source of an appreciable amount of finely divided carbon, and the lubricating oil does not yield that variety of carbon when the gas is used as engine fuel, Part XV (3). Detonation was therefore not obtained when the gas was used even at the unusually high compression ratio of 12 : 1 but surface ignition became evident at maximum power on raising the jacket coolant to 351° F. at a compression ratio of 10 : 1, Part XII (4), or to 295° F. at a compression ratio of 12 : 1, Part XIII (5). Detonation was, however, obtained at the relatively low compression ratio of 9 : 1 on adding finely divided carbon as graphite dust to the entering gas–air mixture, Part XV (3).

Benzene is like town gas in being a nonknocking fuel in ordinary conditions of engine operations, surface ignition but not detonation occurring at high compression ratios as first demonstrated by Ricardo (11, p. 145) when running the E 35 engine at 1500 r.p.m., jacket coolant at 140°F., and with heat added to the entering air at the rate of 1500 watts. The antiknock property is due, according to the nuclear theory, to the difficulty of decomposing the substance to carbon by thermal cracking of the end gas in the time available when it is used as an engine fuel. It is possible, however, as shown by the experiments described in this Part, to provide burning conditions in which benzene in any usable concentration in mixtures with air will provide the finely divided carbon required to induce detonation.

Experimental Conditions and Methods

The benzene used for the experiments was reputed to be free of sulphur. Surface ignition was prevented by running the engine at relatively low jacket coolant and inlet air temperatures and at the unusually low speed of 400 r.p.m. in order to reduce power and consequently the temperature gradient required for heat transfer to the coolant.

The C.F.R. knock testing engine used for the experiments was "standard" except that the shrouded inlet valve was replaced by one of the common tulip shaped variety and the arrangement for measuring compression ratios modified to permit measurement of values extending to 13 : 1. Lubrication was by a commercial S.A.E. 30 oil, without additives. The oil in the crankcase was always maintained at approximately 130° F. by the electric heater provided as standard C.F.R. equipment. Inspection of the cylinder and piston on completion of the engine experiments revealed that no damage from defective lubrication had occurred.

Water was used as the coolant and temperature controlled by the thermostatic device described in Appendix (*b*), Part XIII (5), which made possible the maintenance of a nearly uniform coolant temperature. The water entered the bottom of the cylinder jacket at 85° F. and left the top of the engine head jacket at 90° F.

The air supply was metered by the air box orifice method described in Appendix (*c*), Part XIII (5), the equipment being set up outside the laboratory building but with pressure leads to a manometer inside, near the engine. The temperature of the air as metered was 32° F. and the relative humidity 58%. The metered air passed through 20 ft. of 3 in. bare steel pipe in the warm laboratory and entered the carburetor at a temperature of 67° F. The relative humidity was then 16%.

Carburetion conditions were arranged to ensure that the benzene was present in the mixture with air, at the beginning of compression, in large part as liquid drops. Thus the mixing chamber fitted as standard C.F.R. equipment was removed and the carburetor, without the usual diffuser, bolted directly to the engine head. The benzene then entered the carburetor as a homogeneous liquid jet and it is probable that "spraying" occurred mainly at the inlet valve because of the high mixture velocity necessarily attained. The temperature drop from the inlet to the outlet of the carburetor was from 9° to 15° F. only, indicating that little vaporization had occurred prior to the entry of the benzene into the cylinder.

Ignition Arrangements

Spark advance was set arbitrarily at 30° at 7 : 1 compression ratio. The timing lever was then linked to the movable engine head and advance varied thereafter automatically with compression ratio. Spark advance was accordingly 25° at 13 : 1, the highest compression ratio of the experiments, and 38° at the low compression ratio of 4.8 : 1. The standard C.F.R. ignition system was modified as described in Appendix (*a*), Part XIII (5), and the spark gap set at the usual width of 0.025 in.

Standard Knock Intensity

The bouncing pin contacts were so adjusted that a mid-scale reading on the knockmeter was obtained for the approximate standard audible knock intensity of earlier experiments; pentane being used as the fuel. The intensity may be described as moderately heavy. Standard intensity of knock was then taken as having been attained with benzene on adjusting compression ratio for mid-scale knockmeter reading. *It was especially noticeable that the audibility of knocking combustion with benzene varied over a wide range while intensity as indicated by the knockmeter reading was "standard".*

Measurement of Power and Efficiency

Brake horsepower was measured by a swinging field electric dynamometer and the indicated value obtained by the motoring method in general use. Corresponding values of mean effective pressure can be obtained by multiplying by the factor 53.1. Corresponding values of indicated or brake thermal efficiency are based on benzene having a lower calorific value of 17190 B.t.u. per lb.

Experimental Results

The experimental results are exhibited by the graphs of Fig. 1, values of the compression ratio for standard knock intensity, brake and indicated horsepower, and brake and indicated thermal efficiency being plotted as ordinates on a base of mixture strength values. The compression ratio for

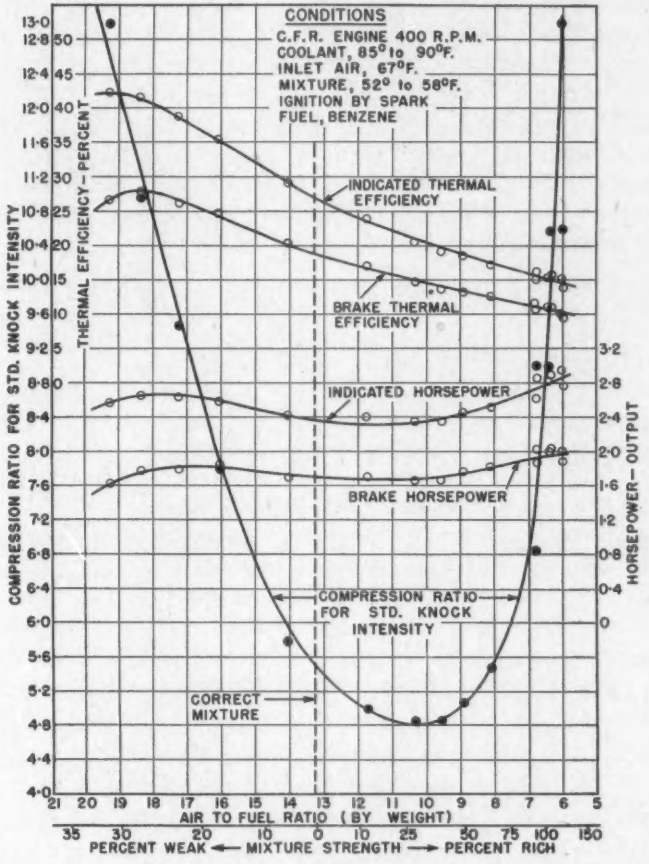

FIG. 1. *The variation of standard knock intensity, power, and thermal efficiency with mixture strength when using benzene in conditions to promote nuclear ignition.*

standard knock intensity may be regarded as the usable value for the mixture strength at which it is determined and will be referred to as U.C.R. It will be seen by reference to Fig. 1 that it varied from the very low value, for benzene, of 4.8 : 1 for a mixture 30% rich to the high value of 13 : 1 for a mixture 31% weak or 120% rich. Arrangements to use compression ratios higher than 13 : 1 had not been made.

The experiment was begun with a nearly clean combustion chamber and a mixture 5.5% weak. The U.C.R. as indicated by a mid-scale reading of the knockmeter was then 5.8 : 1 although audible intensity was very light. Mixture strength was increased by steps, and corresponding values of U.C.R. determined, as indicated by mid-scale knockmeter readings, until the maximum measurable value of 13 : 1 for the compression ratio was attained. The mixture was then 120% rich. The audibility of knock increased progressively with increase of mixture strength and at the compression ratio of 13 : 1 was nearly the same as that usually associated with mid-scale knockmeter reading.

The series of measurements was interrupted at a U.C.R. of 10.6 : 1 by the sooting of the spark plug. The part of the combustion chamber, mainly the piston crown, visible through the spark plug hole was then inspected with the aid of interior lighting. The surface was seen to be heavily coated with powdery carbon of the lamp black type.

The experiment was resumed after fitting a clean spark plug and four check observations taken over the mixture range 120% to 90% rich and completed on taking four observations when using mixtures in the order 23%, 31%, 17%, and 28% weak. Audible knock intensity for the mixtures 23% and 31% weak was the same as that observed for very rich mixtures. Intensity diminished progressively for the third and fourth observations but was accompanied by occasional heavy knock. Compression ratio was adjusted for all of the observations to maintain standard knock intensity as indicated by a mid-scale reading of the knockmeter.

Inspection through the spark plug hole on completion of the experiment revealed a thin layer of carbon black on the piston crown. The layer was reduced but not completely removed on continued running of the engine with a mixture 30% weak. Thus it appeared that the layer of powdery carbon on the piston crown formed when running on very rich mixtures diminished in thickness with time of running on changing over to weak mixtures.

It is significant in view of developments to be described later that on switching off the electric spark the engine did not continue to run in the temperature and other conditions of the experiments.

A selection of significant data from the experimental results is given in Table I.

TABLE I

VALUES OF USABLE COMPRESSION RATIO, POWER, AND EFFICIENCY, FOR SIGNIFICANT VALUES OF MIXTURE STRENGTH

Mixture	U.C.R.	I.H.P.	I.M.E.P.	I.T.E.
31% weak	13 : 1	2.56	137 lb.	42%
Correct	5.5 : 1	2.36	125 "	27%
28% rich	4.8 : 1	2.35	125 "	21%
60% rich	5.3 : 1	2.48	132 "	18%
120% rich	13 : 1	2.96	157 "	15%

Discussion

The experiments were carried out in cool engine running conditions in order to prevent surface ignition and simultaneously to promote the burning of benzene in a manner to yield finely divided carbon as soot. The manner in which finely divided carbon is procured remains to be considered.

It is well known that the flame of benzene in an atmosphere deficient in oxygen deposits soot on available surfaces to a greater extent than that of a substance, hexane for example, which contains the same number of carbon atoms in the molecule but more than twice as many atoms of hydrogen. Benzene is thus an undesirable constituent of lamp oil, and readily deposits carbon in the combustion space of an engine when rich mixtures are used. Carbon can however be formed even when oxygen is in excess and combustion complete at the *end* of the period required in an engine, if liquid drops have persisted throughout compression to be present at the *beginning* of the period, when flame is started by the electric spark. The temperature conditions of the engine experiments ensured that the combustible mixture contained sufficient benzene as vapor for spark ignition and sufficient as liquid drops to provide the locally rich mixtures required for the formation of soot. When the mixture in the engine contains an excess of benzene, carbon would be formed on the impingement of the flame on relatively cool surfaces as well as by the burning of liquid drops in the gaseous mixture. When the mixture contains an excess of oxygen, carbon would be formed only by the burning of the locally rich mixture adjacent to the droplets.

The carbon formed as described was always of the powdery lamp black type which could be dispersed into the mixture by the turbulence created by the restriction of the inlet valve, and in the light of the nuclear theory a rational explanation for the characteristics of the detonation observed in cool conditions of engine operation is thus obtained.

Some comment is required in respect of the measurement of knock intensity when using benzene as an engine fuel. It was observed, by King and Moss, in the course of early experiments on "The Measurement of Detonation" (8, p. 220) that the bouncing pin method was not satisfactory if used over a wide range of compression ratios. Although audible knock was not obtained when benzene was used in the experimental conditions, the effect was indicated by the bouncing pin as existing at a compression ratio of 6 : 1 but not at 4 : 1. In another experiment in which there was again no *audible* knock with benzene, the bouncing pin contacts were set just not to indicate any effect. Then on changing to gasoline, knock was plainly audible although no indication of it was given by the bouncing pin. It is evident that the knocking combustion of benzene differs in some way from that of paraffinic fuels. The reason for the difference might be of importance but so far as known has not been ascertained.

Acknowledgments

The experimental work was carried out in the Heat Engine Laboratory of the University of Toronto with the co-operation of Prof. E. A. Allcut, Head of the Department of Mechanical Engineering, and that of Assistant Professor W. A. Wallace, and the cost defrayed in part by an extramural grant from the Defence Research Board (Canada). Experimental assistance was given by Mr. S. Sandler of the Defence Research Board Group in the Department of Chemical Engineering.

References

1. KING, R. O. Can. J. Research, F, 26 : 228-240. 1948.
2. KING, R. O. and DURAND, E. J. Can. J. Research, F, 27 : 337-346. 1949.
3. KING, R. O., DURAND, E. J., and ALLAN, A. B. Can. J. Research, F, 28 : 177-188. 1950.
4. KING, R. O., DURAND, E. J., and MORRISON, J. ALEX. Can. J. Research, F, 27 : 435-449. 1949.
5. KING, R. O., DURAND, E. J., WOOD, BERNARD D., and ALLAN, A. B. Can. J. Research, F, 28 : 134-155. 1950.
6. KING, R. O. and MOLE, G. J. Inst. Petroleum Technol. 20 : 130, 791-820. 1934.
7. KING, R. O. and MOLE, G. J. Inst. Petroleum Technol. 21 : 144, 838-859. 1935.
8. KING, R. O. and MOSS, H. Engineering, 128 : 219-221, 272-274. 1929.
9. KING, R. O., WALLACE, W. A., and DURAND, E. J. Nature, 163 : 729. 1949.
10. KING, R. O., WALLACE, W. A., and MAHAPATRA, B. Can. J. Research, F, 26 : 264-276. 1948.
11. RICARDO, H. R. Proc. Inst. Automobile Engrs. (London), 18. Part I. 1923-24.

A REMOTE CONTROL PROJECTOR FOR THE EXAMINATION OF EXPERIMENTAL RECORDS ON 35 mm. FILM[1]

By E. L. R. Webb

Abstract

A projector unit is described in which the film advance sprocket is driven by a reversible motor and the glass pressure plate is automatically released while the film is being moved. The film spools accommodate 100 ft. of 35 mm. film and take up slack in both directions. Several units may be used simultaneously for correlation of multiple records.

Introduction

This projector was built originally to do one specific job for which there was no known commercially available equipment, but it has proved satisfactory in many other applications in our laboratories. Wherever large amounts of 35 mm. film are exposed in other than conventional motion picture cameras there is need for a special projector to examine the record. In experiments where the quantity to be measured is not already electrical in form, there is a general tendency to convert it to an electrical equivalent, for ease of transmission and/or amplification. To record signals varying faster than a moving pen instrument can follow, a popular technique is to photograph the screen of a cathode ray oscillograph. The resulting records fall into two general classes, either discrete pictures, as in a sequence of shots of the P.P.I. presentation of a radar set, or continuous time graphs. The latter may be further subdivided into wavy line records, traced either along or across the film by a deflection modulated spot, and scanned records produced by a brightness modulated scanning spot. It was for the detail examination of distance–time records of the last type that the projector was developed in connection with meteor-echo research. When three or more stations are operating simultaneously each with a camera exposing film at a few inches per minute (or even per second sometimes) the reduction of the data is greatly facilitated by the use of a battery of these special projectors.

Description

The over-all requirements for the projector are: it must handle 35 mm. film on standard spools and in lengths up to 100 ft.; it must project a given portion of film indefinitely without burning or other ill-effect; controls must be provided for advancing the film smoothly, by any amount and in either direction; the film must move and stop rapidly to avoid wasted time in going from one spot to another, but while in motion the projected picture must still be readable for scanning purposes.

[1] *Manuscript received April 21, 1950.*
Contribution from the Division of Radio and Electrical Engineering, National Research Laboratories, Ottawa, Canada. Issued as N.R.C. No. 2177.

The optical components used were those from a combination slide and film projector made by the Society for Visual Education. Their model AAA projector has a good optical system consisting of a 300 w. projection lamp, a three element condensing system, a heat absorbing filter, glass pressure plates for unmounted film, and a high quality projection lens. A selection of focal lengths is available, the 5 in. being used normally. The extra features required could not be hung on the projector frame, and so a new machine was designed that incorporated the modified S.V.E. projector as a component part. Complete detail and assembly drawings were made in the course of the design so that additional units could be shop built at a future time. Despite the extensive modifications to the original projector to facilitate handling film on 100 ft. spools, the slide changer may still be replaced and used to show 2 in. by 2 in. slides.

The main frame or chassis of the modified projector is an $\frac{1}{8}$ in. aluminum sheet about 12 in. by 9 in. To this are bolted the projection-lamp/condenser-lens system behind, and the film holder and projection lens in front; the electric motor and gears to drive the film sprocket; the electromagnet mechanism for releasing the pressure on the backing plates while film is being moved; the supply and take-up spool spindles, on separate brackets; the take-up motor together with its gears and clutches; the terminal block for electrical connections and lastly the supporting legs. Two electric cords are attached—one to plug into 110 v., 60 cycles service, the other for remote control switch.

The S.V.E. model AAA projector is so built as to allow the film strip holder and the projection lens to be rotated 90° about the optical axis. This is to ensure that scenes taken with the camera held either vertically or horizontally may be projected right side up. In our projector the horizontal position only is required, so the rotation bearing (which was very conveniently $\frac{1}{8}$ in. thick along the optical axis) was discarded and the two halves of the projector are mounted on either side of the $\frac{1}{8}$ in. aluminum chassis.

The rear half of the projector containing the light source was modified only to the extent of leaving off the base containing the tilt mechanism and rubber mounting feet. The front half of the projector had several modifications. The original film supply and take-up arrangement would handle only a few feet of film, so it was cut away leaving only enough of the ferrotype guides as would be required to guide and protect the film in the final assembly. The original film transport mechanism consisted of a sprocket, operated by a hand knob, which in turn released the pressure of the film backing plate by means of a cam. The cam was also arranged to act as a detent device so that the film could be moved either a single or double frame at a time. The pressure release cam was eliminated and replaced by an electromagnetic device. The hand knob shaft was replaced by a shaft extending below and carrying a miter gear (Boston G464) whose mate is on the shaft of a Bodine KCI-22 motor. The motor was mounted by means of a bracket to the aluminum chassis.

The film backing plate linkage was modified and extended to connect with the electromagnetic portion of a Leach No. 6104 relay, from which the contact assembly had been removed. The magnet closed a little too aggressively when energized for the normal 110 v. a.c. and attempts at inserting dampers, etc., amounting to mechanical low-pass filters, were not fruitful. Reducing the a-c. voltage led only to severe chattering. However, it was found that the magnet closed firmly and quietly when energized by about 20 v. d.c., so a power supply was added, consisting of a small transformer, selenium rectifier, and large filter condenser (2000 μf.). By using such a large condenser and by switching in the transformer primary, the closing of the magnet motor was made quite slow, also the opening was delayed after switching off. The delay was about the same as the coasting time of the film transport motor. Thus the pressure was not applied until the film stopped. A useful feature of this delay action is apparent when several quick starts, stops, and reversals are being made in the process of centering up an interesting part of the film, since the pressure plate magnet operates at the beginning and releases again only at the end of the switching sequence. It should be mentioned that there is a slight tendency to defocus while the film is unclamped. It is always possible to readjust the lens slightly so that the film is in good focus for continuous scanning, if that mode of operation is being used.

The supply and take-up spools are standard Eastman 35 mm. 100 ft. reels. Each spool engages a pin on a spindle mounted vertically on a sheet metal bracket which is in turn bolted to the aluminum chassis. In normal operation the film may be moved backwards as well as forwards and so the functions of supply and take-up spools become interchanged. Of the several possible arrangements of one or two motors, clutches, brakes, etc., the method selected was to gear one motor to both spindles in such a way that each spindle always turns in the direction to wind up. The speed of each spindle is greater than the minimum required to take up all slack at all times, and the spools are connected to their respective spindles via friction clutches. Thus the "take-up" spool slips on its spindle and the "supply" spool turns backwards on its spindle. The take-up drive motor (similar to the sprocket motor) is energized in parallel with the film pressure-release magnet-motor and so operates only when the film is being moved. Five miter gears (Boston L95) are used to connect the motor and two spindles. There are three supporting legs fabricated of sheet metal and bolted to the chassis. The leg directly under the lens has a screw adjustment for tilting the projector. A barrier terminal strip serves as a tie point for the various plug cord, lamp, motor, and control circuits.

The various electrical components are connected as shown on the wiring diagram, Fig. 1. The over-all assembly is shown on the illustration drawings, Fig. 2.

The motors and gear ratios were selected, after considerable experimentation, to provide a film speed of 30 in. per minute. At this speed continuous scanning

of the moving film can be done without serious eye strain. If different film speeds are desired, there are two optional modifications. First, the film transport spindle miter gears may be replaced by bevel gears with the disadvantage of incorrect take-up reel speed. Second, both Bodine motors

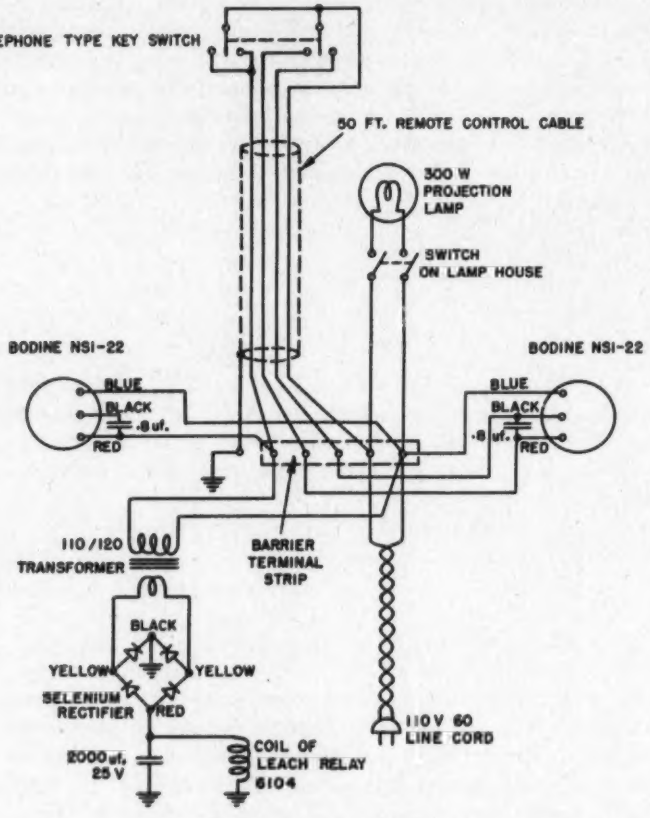

FIG. 1. *Wiring diagram.*

may be replaced by units having identical exterior dimensions but whose output shafts turn at a new speed. It is possible that at high film speeds some form of braking might be desirable to cut down the film stopping time, though an experienced operator can stop the film almost instantly by a touch of "reverse throttle".

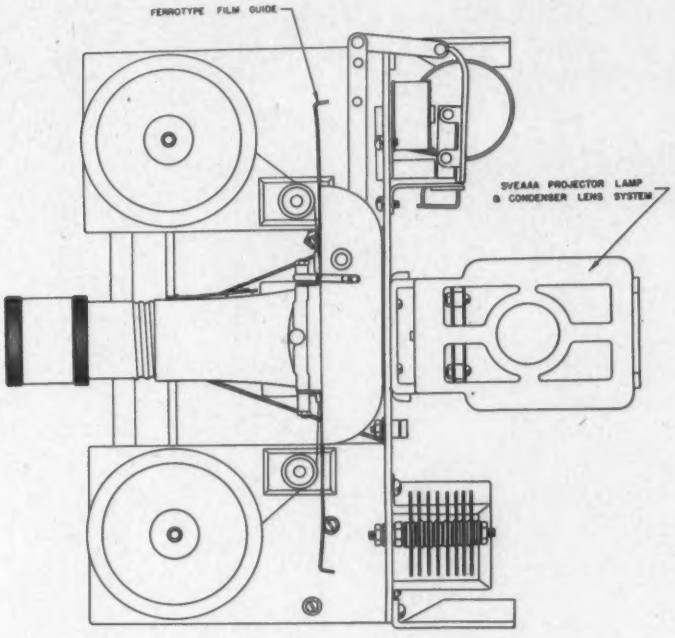

FIG. 2. *Plan and elevation views of 35 mm. motorized projector.*

Two auxiliary devices have proved useful in our work. One is simply a hand-operated rapid rewind machine, as shown in Fig. 3. The other is a direct film viewer (Fig. 4) wherein a 3 ft. length of the 35 mm. film is seen

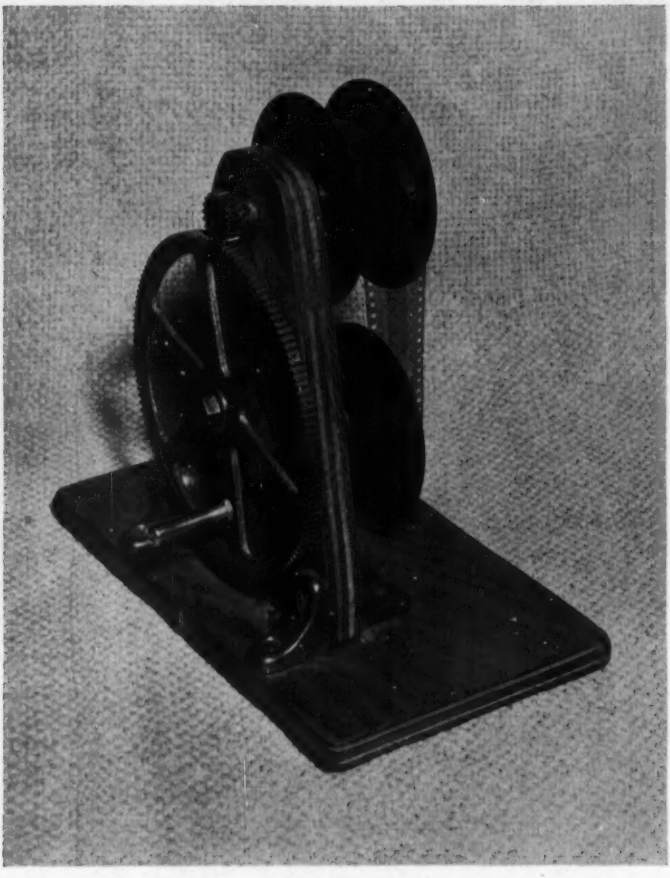

FIG. 3.

against a bright background provided by a fluorescent lamp. This device also is hand-driven and is of value in locating quickly any "special interest" portions of long films which may then be transferred immediately to the projector. Both the direct film viewer and the projector can be easily loaded or unloaded anywhere in mid-film.

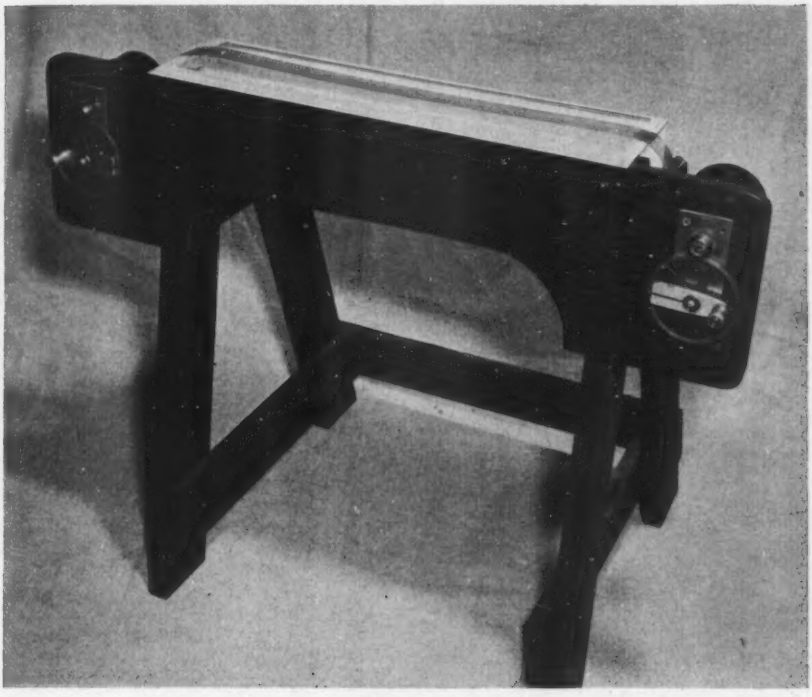

FIG. 4.

Applications

In addition to the original application the projector has been used as a printing enlarger for fairly large blow-ups. When used in this service an external shutter-iris-filter assembly is added. This consists of a set of swinging flaps mounted in front of the projection lens. A red gelatin filter is mounted in one flap, interchangeable inserts with various apertures fit into another to form the iris, and a third plain flap acts as shutter. The enlarging paper is either pinned to the screen, or, if a large number of prints are being made, a magazine holder for the printing paper may be used.

In our installation a room has been subdivided into a projection booth, a dark room, and a drying room. The last two contain conventional equipment for processing 35 mm. film and large prints. The projection booth however is a little unusual. It is long and narrow, with the main screen permanently mounted on one end wall. Overhead tracks are mounted along the ceiling and from these is suspended a sturdy carriage with three decks. On each deck is a complete projector, as seen in Fig. 5. The power supply is carried through a flexible cord to convenient outlets at each deck. The individual

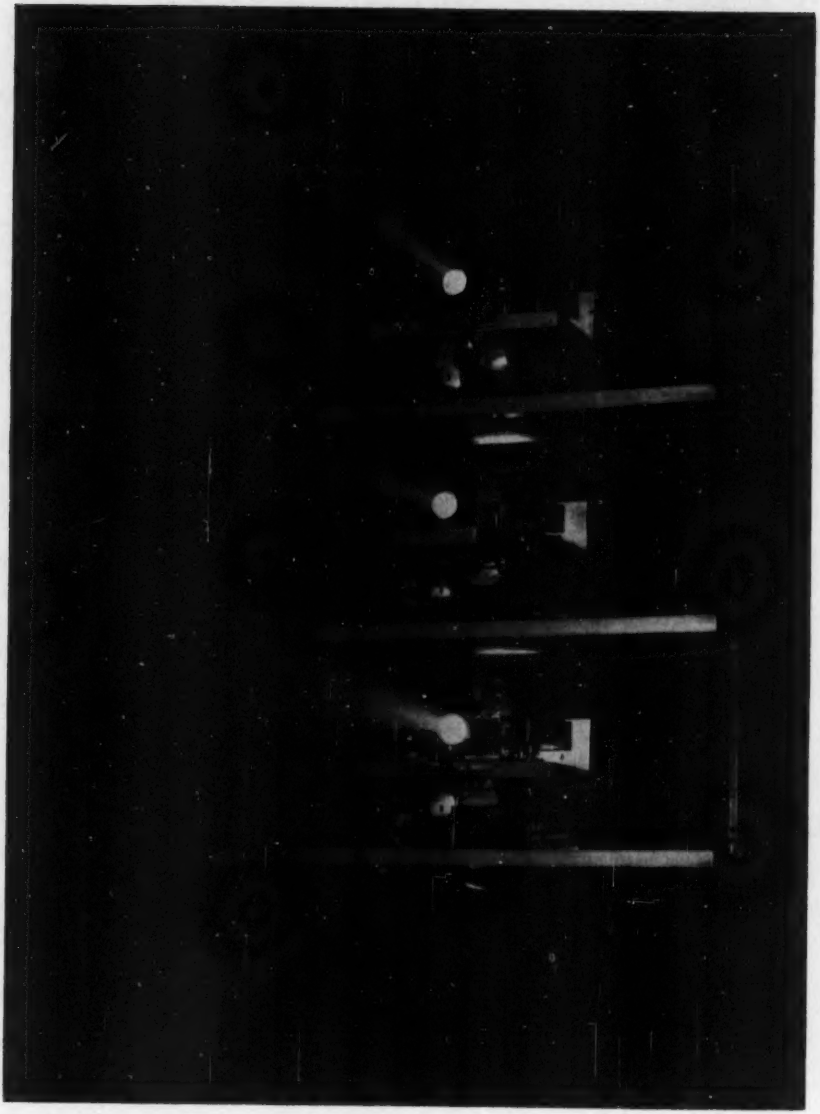

FIG. 5.

control cables are carried along the wall to the viewing position. The operator sits in a one-armed lecture room chair. On the arm is fastened a small box containing three telephone type switches arranged for one hand operation. The switches are spring loaded so that they return to the center or neutral position when released. The control cords plug into the box separately, allowing any projector to be removed without disturbing the remainder.

The projectors have been used so that the middle one only throws a picture on the center of the screen, or the top and bottom ones throw a pair of pictures one above the other, or all projectors together, a stack of three pictures. By adjustment both of the carriage position and of the individual leveling screws, suitable enlargements and screen coverage can usually be achieved in every case.

Our chief use for two-projector operation is the reading of the separate records from a radar set and a Doppler equipment for meteor-velocity determinations. Time, measured to a small fraction of a second, is the correlating factor. All three projectors are used when examining records from three independent radars for "triple-coincidence" data to be used in triangulation. There have been occasions when four or more projectors would have been handy.

The original projector has been in continuous use for 18 months; the others were put in service a few months later. Several groups working on different projects have used the equipment. Sometimes the middle projector has been reversed on its stand to project on the rear wall and so to allow two observers to work independently.

One or more of the projectors have been used in lecture halls for illustrated talks. The remote control cable was extended so that the speaker could operate the projector from his position near the screen, ensuring smoother operation than is usually achieved with an assisting projectionist.

THE CURVE COMPUTER[1]

By W. E. Knowles Middleton

Abstract

An electromechanical instrument has been developed, which adds, subtracts, multiplies, or divides the ordinates of two curves in Cartesian co-ordinates, plotting the resulting locus. This uses the principle of the Wheatstone bridge, and is semiautomatic; the curves are followed manually, but a phase-sensitive servo system keeps the bridge in balance. Attachments are provided for determining the area under the resulting curve, and also for the performance of certain logarithmic operations of interest in photometry. In the ordinary use of the computer, the accuracy is about 0.3% of full scale or better.

1. Purpose and Principle of the Curve Computer

The instrument to be described in this paper, while clearly of some general interest, was originally conceived in an effort to reduce the very considerable labor of calculating optical filters for the correction of phototubes and other similar purposes. Once the manner of performing the elementary operations was determined, other uses in colorimetry and elsewhere naturally suggested themselves, and led to certain modifications and additions.

The curve computer may be described briefly as an electromechanical device, operating on the principle of the Wheatstone bridge, which adds, subtracts, multiplies, or divides the ordinates of two separate Cartesian curves, and plots the resulting locus. Attachments make it possible to perform certain logarithmic operations, and to determine the area under the plotted curve.

The principle of the Wheatstone bridge has been applied to computation before, for example by Ergen (1). Its remarkable simplicity and versatility render it attractive for such purposes.

Let us suppose that we have three variable resistors r_i that can be made proportional to three scalar quantities y_i ($i = 1, 2, 3$). Figs. 1*a* to 1*d* show how these may be combined in a bridge with one or two constant resistors K_1, K_2 to perform the four fundamental operations of arithmetic. For addition and subtraction it is necessary that $r_1/y_1 = r_2/y_2$; for multiplication and division even this restriction is unnecessary.

It is possible to work with other than linear functions if we provide some mechanical means of establishing the desired relationship between r_i and y_i.

2. General Description

The way in which this simple principle is applied to Cartesian curves is shown in Fig. 2. Three sheets of similar graph paper are fastened to a table T,

[1] *Manuscript received May 4, 1950.*
Contribution from the Division of Physics, National Research Council, Ottawa, Canada. Issued as N.R.C. No. 2180.

in such a way that the lines $y_i = 0$ are collinear, and so that the spacing between the lines $x_i = 0$ is equal to the common spacing between the tracks of the indexes I_1 and I_2 and the pen P. Thus if the table is moved from right to left, I_1, I_2, and P will have the same x co-ordinate on the three graphs at any given instant.

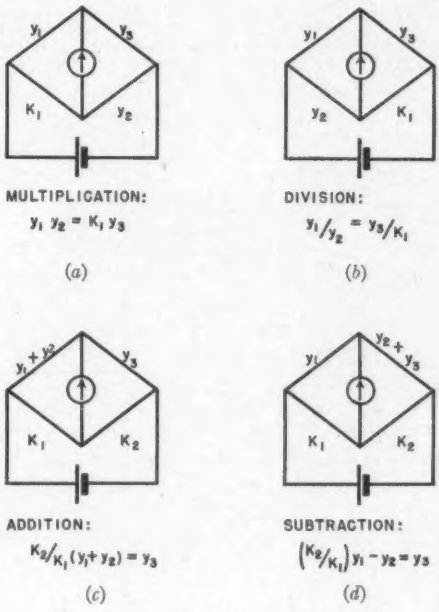

FIG. 1.

The indexes and the pen are driven by flexible stainless steel rope passing over accurately turned pulleys. On the shafts of the three front pulleys are precision variable resistors R_1, R_2, R_3, the angular motion of which is accurately proportional to y_1, y_2, and y_3 respectively, so that we may write

$$r_i = R_i\, y_i.$$

These resistors are linear to $\pm 0.1\%$, and are chosen so that their total resistances are very nearly equal.

R_1 and R_2 are driven through gearing in one of two ways; either by the handwheels Y_1 and Y_2 (Fig. 3), or by a variable-speed drive, the power for which is supplied by the motor M which traverses the table. The details of this drive are not shown, but its rate is controlled for each of the two resistors by the handwheels D_1 and D_2. If these are set, with the clutches C_1 and C_2 in the proper positions, the indexes I_1 and I_2 will describe straight lines of some slope between -10 and $+10$ which can be read on the scales G_1 and G_2 (Fig. 2)

Curved lines are followed by changing this slope continuously with D_1 or D_2, or alternatively by means of Y_1 and Y_2 directly, according to the preferences of the operators.

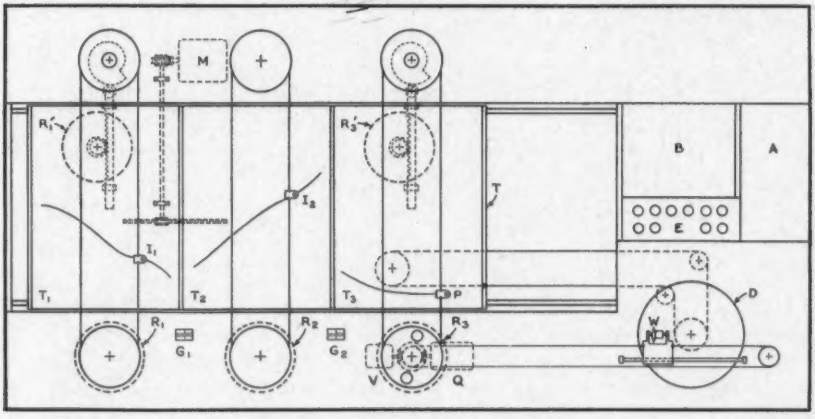

FIG. 2.

The resistor R_3 is driven by a servomotor V, the direction of rotation of which is determined by the out-of-balance current of the Wheatstone net, acting on a phase-sensitive amplifier A. A slight amount of feedback is provided by coupling a direct-current generator Q to the servomotor V, the output of Q being fed through a resistor to the input of the amplifier, with such a polarity that it opposes the out-of-balance current of the network.

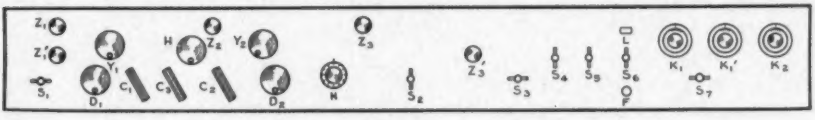

FIG. 3.

The method of dealing with logarithmic functions is also indicated in Fig. 2. R'_1 and R'_3 in this figure denote two additional linear variable resistors, similar to R_1, but driven by rack-and-pinion motions. The racks are displaced by the cams shown in the figure. These rotate through an angle proportional to y_1 and y_3 respectively, and are shaped in such a way that $r'_1 = R'_1 \cdot 10^{-y_1}$ and $r'_3 = R'_3 \cdot 10^{-y_3}$. The switches S_1 and S_3 (Fig. 3) select either the linear or the "logarithmic" variable resistor.

The "fixed" resistors denoted by K_1 and K_2 in Fig. 1 are actually adjustable, 10-turn resistors. K_1 may be either of two such resistors K_1 or K'_1 (Fig. 3) according to the setting of switch S_7. This makes it possible to have two multiplying constants instantly available, frequently a great convenience.

The area under Curve 3 can be integrated by means of the disk D and the wheel W (Fig. 2). The disk is driven by a stainless steel rope fastened to the table T; the radial position of the wheel is determined by another cable passing round a pulley on the shaft of R_3, and is therefore linear in y_3. The wheel has the usual planimeter dials.

3. Mechanical Details

The instrument is built in and on a chassis 48 in. long, 24 in. wide, and 6 in. high. Fig. 4 is a photograph of the complete apparatus.

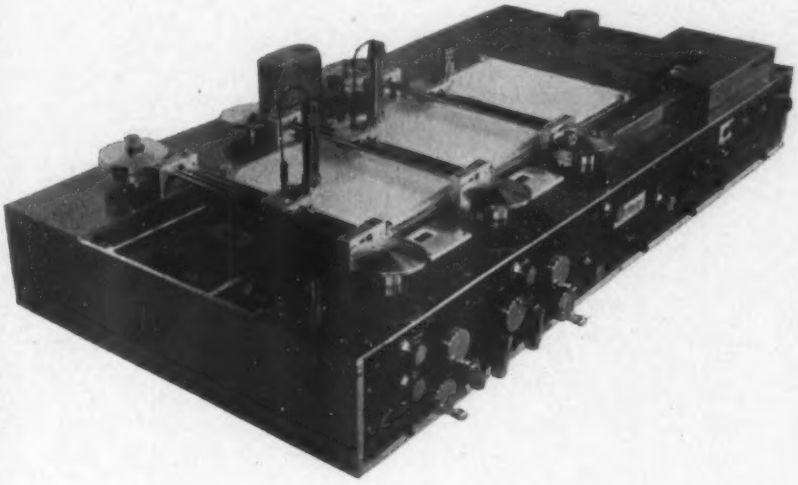

FIG. 4.

The table can be moved sideways in its own plane either manually by a handwheel H (Fig. 3) or by a variable-speed motor provided with a reverse gear. Each part of the table is furnished with four spring catches for holding sheets of paper of the usual letter size, 8½ by 11 in. A low fence determines the position of the left-hand edge of each sheet, and an engraved line parallel to the front edge of the table serves as a permanent reference line for $y = 0$.

The carriages for the pointers I_1 and I_2 and the pen P roll on cylindrical ways, small ball bearings being used to provide almost frictionless rollers. The pointers are optical, each consisting of an illuminated graticule, a green filter, and a lens, and project small crosses of green light on to the table. This entirely avoids the possibility of parallax in following curves. The penholder is mounted in such a way that it can be rotated into three positions. In one, the pen is held entirely off the table; in the second, it is held up by a light spring but can be depressed to make a dot; in the third, it rests on the table.

Zero adjustments are provided for the variable resistors by means of knobs Z_1, etc. (Fig. 3), and it is also possible to adjust the planimeter wheel W (Fig. 2) in relation to the position of the pen.

The inverter-amplifier and servomotor are of a standard type manufactured by the Minneapolis–Honeywell Co. for their recording potentiometers. The battery for the bridge is a $22\frac{1}{2}$ v. "C" battery, with numerous taps. About 12 to 15 v. is actually used.

Limit switches are provided which stop the drive motor if either the table or the indexes reach the end of their travel. No limit switches are needed on the pen carriage, as the servomotor can be stalled without damage.

4. Operation

There is no need to enter into all the details of operation of the Curve Computer, and we shall discuss only a few points of special interest.

The preliminary adjustment of the zeros of the resistors is best made with an ohmmeter, terminals being provided at E (Fig. 2) for its connection. This applies especially to R_1' and R_3'. It is, however, possible to adjust the zeros by trial and error without auxiliary apparatus. When the zeros have been adjusted, the switch S_4 may be set to "multiply", and the indexes both set to whatever values of y are considered unity (usually the top of the sheet of graph paper). If the power is on, the pen will then take up some position or other. The resistance K_1 is then adjusted until the pen indicates unity, expressing the multiplication $1 \times 1 = 1$. This process is valid even if the various sheets of graph paper are of different sizes, and in this sense the instrument is self-calibrating. A similar process may be used for division, since $1 \div 1 = 1$. Naturally we may introduce any constant within reason by suitable adjustment of K_1.

To adjust the curve computer for addition or subtraction, the above adjustment for multiplication is made first; the instrument then being set to add, for example, I_1 and I_2 are each set to $y = 0.5$, and the value of K_2 adjusted until the pen indicates $y_3 = 1$, K_1 being left as it was. In this instance it is important that the three sheets of graph paper should be identical, but their dimensions are otherwise restricted only to a maximum value $y = 10$ in.

If logarithmic operations are contemplated, however, the resistors R_1' and R_2' must be adjusted for the particular scale of the paper. In practice they are left adjusted for a log unit of 10 in.

It is not difficult to learn to follow curves. When using the rate drives, one can develop the feeling of driving a car along a winding road, and make small corrections almost unconsciously. When the instrument was first designed it was hoped that one operator would be able to follow two curves simultaneously; but this is not practicable. A surprising number of operations involve only one curve and a constant, but where two functions have to be multiplied, etc., two operators are required.

5. Typical Operations with Transmittance Curves

One of the most obvious uses of the curve computer is to predict the results of combining filters. Since the transmittance of n filters in series is the product of the transmittances of the individual filters, the spectrophotometric curves of two filters may be placed on tables 1 and 2 and multiplied directly. If there are further filters this result may be multiplied by the transmittance of the next one, and so on.* If a recording spectrophotometer is available, the original curves may be used.

The curve computer may also be used to predict the results of altering the thickness of a filter. The simple theory of this is given, for example, by Gage (2). It is first necessary to work out the "internal" density D' of the given filter (*not* including the effect of reflection from the surfaces). If T is the transmittance at a given wave length, then the internal transmittance T' is

$$T' = T/p,$$

where

$$p = 1 - 2\left(\frac{n-1}{n+1}\right)^2,$$

n being the index of refraction of the glass (3, p. 411). For most filters p is about 0.92. Further,

$$10^{-D'} = T' = T/p\,.$$

If then we put the T curve on table 1, set index I_2 at p, set S_3 to use the logarithmic resistor R_3', and divide, the pen will draw a curve of D'. This curve may then be transferred to table 1, and multiplied or divided by any desired constants, producing a family of internal density curves for filters of the same glass but of various thicknesses. To re-convert these into curves of transmittance, they are placed on table 1 and the switch S_1 set to use the logarithmic resistor R_1'. Since

$$T = p\ .10^{-D'}$$

the values of T will be plotted by the pen if we set I_2 at p, S_3 to use the linear resistor R_3, and multiply. If we have to go outside of one log unit of density (i.e., if $T' < 0.1$), a second log unit is available by the use of K_1' and S_7, as explained above.

6. Correction of Reflectance Curves

In the operation of a commercial recording spectrophotometer, it is generally necessary to correct for departures of the reference surface of magnesium oxide actually used from the best possible magnesium oxide surface. Such corrections may be conveniently made by running a curve for a standard sample of white opaque glass. If a number of test samples have been measured, the calculations involved may be made with great rapidity on the curve computer by

* *This does not, of course, allow for inter-reflections. The error from this cause is seldom important for filters which attenuate by absorption but may be significant in special cases.*

first determining the ratios between the ordinates of the curve for the white glass sample and a curve plotted from its precisely determined reflectances. (This curve may be preserved for future use.) Each spectrophotometric curve is then multiplied by the curve representing these ratios.

7. Example of a Nonspectrophotometric Problem

In the theory of a certain instrument there occurs the quantity

$$\int_0^{\pi} \beta'(\phi) \sin \phi \, d\phi ,$$

where $\beta'(\phi)$ is a scattering function and is nonanalytic. The instrument is supposed to integrate from 0° to 180°, but for technical reasons it is impossible to reach either limit. It is easy to find the relative error produced by the neglect of any given angle at either or both ends of the range. If $\beta'(\phi)$ is plotted against ϕ on one sheet, $\sin \phi$ on another, the curves may be multiplied on the curve computer, stopping the table at each of the desired values of ϕ near each end and reading the integrating wheel.

8. Accuracy of the Curve Computer

In discussing the accuracy of this instrument, it is of course necessary to distinguish the errors of the electrical and mechanical components, those of the graph paper used, and those of the operators who have to follow the curves. We may dismiss the subject of the graph paper very briefly by stating that modern graph paper of the best quality will introduce no important errors, provided that all the three sheets are from the same plate, and are in humidity equilibrium with the air in the room.

Instrumental errors may occur: (*a*) because of nonlinearity of the variable resistors R_1, etc.; (*b*) in addition and subtraction, because of dissimilarity between R_1 and R_2; (*c*) in logarithmic operations, because of errors in the cam mechanisms; (*d*) because of the finite speed of response of the pen mechanism.

It turns out that the linearity of the resistors is very good. If adjustments are carefully attended to, no error greater than 0.02 in. ($\Delta y = 0.002$ for the unit of 10 in.) should occur in multiplication or division because of departures from linearity. The sort of accuracy obtained in addition is shown in the following Table I.

TABLE I

SPOT CHECKS OF ADDITION

y_1	y_2	y_3 (exper.)	Error	y_1	y_2	y_3 (exper.)	Error
0.4	0.5	0.900	0.000	0.5	0.2	0.700	0.000
0.3	0.5	0.800	0.000	0.5	0.1	0.601	+0.001
0.2	0.5	0.700	0.000	0.1	0.1	0.205	+0.005
0.1	0.5	0.600	0.000	0.2	0.2	0.402	+0.002
0.05	0.5	0.552	+0.002	0.3	0.3	0.601	+0.001
0.5	0.5	1.000	0.000	0.4	0.4	0.801	+0.001
0.5	0.3	0.801	+0.001	0.8	0.2	1.000	0.000

In logarithmic operations, the cams are also involved. Table II shows the result of setting switch S_3 to "log", and multiplying various values of y_1 by 1.00. The most probable cause of these moderate errors is a slight eccentricity of the pinion which rotates the variable resistor.

TABLE II

SPOT CHECKS OF LOGARITHMIC PROCESS

y_1	y_3 (calc.)	y_3 (exper.)	Error
0.1	1.000	1.000	0.000
0.2	0.699	0.693	−0.006
0.3	0.523	0.518	−0.005
0.4	0.398	0.393	−0.005
0.5	0.301	0.298	−0.003
0.6	0.222	0.220	−0.003
0.7	0.155	0.154	−0.001
0.8	0.097	0.096	−0.001
0.9	0.046	0.045	−0.001

The servo system driving the pen mechanism reaches its limiting speed with a very small input voltage. Because of this, there is almost no lag in the response of the instrument up to a certain critical pen speed. Actually this speed corresponds to a curve with a slope of more than ±12 at the lowest table speed, and is seldom attained in actual operation. Any curve which is suspected of having an appreciable error from this cause can be checked by plotting one or two points with the table stopped. As an indication of the speed of following, the instrument will go up and down a straight line of slope 8 (by reversing the table) with almost no thickening of the line. It would be perfectly feasible to gear up the servomotor, which has ample power, to give the pen at least four times its present maximum speed.

The best indication of the precision of curve following by the operators is probably the standard deviation of repeated integrations of the area under the same product curve. As an example, the reflectance curve of a bright red paint, which has a steep portion in the middle, was multiplied by a constant and the product integrated. The standard deviation of a single integration was 0.15%. The nine product lines, drawn in this instance with a fine pencil, formed a uniform band about 0.05 in. to 0.07 in. wide.

Naturally the multiplication of two curves is somewhat less precise. The curve referred to above was multiplied nine times by a curve representing the function $E_c\,\bar{y}$ familiar to colorimetrists. This is a curve shaped much like a probability curve. The integrated product (which gives the total visual reflectance of the color in daylight) had a standard deviation of 0.5% (for a single integration). This was probably a fairly severe test, because of the presence of a region where one curve was ascending steeply, the other in equally rapid descent.

9. Possible Developments

The curve computer has now been in service for about five months, and has shown no serious defects. Probably the chief desideratum is a change in the gear ratios between the handwheels Y_1 and Y_2 and the corresponding pointers. Manual following would be easier if these were geared down several times, but unfortunately this would involve taking a great deal of the instrument apart, and has not yet been attempted.

If there should be any demand for such a feature, an instrument could easily be constructed which would plot the squares of the ordinates of one curve. This would involve mounting two linear variable resistors on one of the shafts, each having a separate zero adjustment. Another possibility, much simpler to put into practice, would be the provision of terminals for the connection of external resistors in series with R_1, R_2, and R_3. This would greatly extend the range of linear operations possible with the instrument.

Acknowledgments

It is a pleasure to acknowledge the enthusiastic co-operation of Mr. F. W. Freeth, Superintendent of Workshop Services, and of a number of his highly skilled staff.

Thanks are also due to Miss Eleanor G. Mayo and the staff of the Photometry and Colorimetry Section for aid in the testing of the instrument.

References

1. ERGEN, W. K. Rev. Sci. Instruments, 18: 564-567. 1947.
2. GAGE, H. P. J. Optical Soc. Am. 27: 159-164. 1937.
3. WOOD, R. W. Physical optics, 3rd ed. The Macmillan Company, New York. 1934.

FLOWMETER ERROR IN MEASURING PULSATING FLOW[1]

By G. W. C. TAIT[2]

Abstract

Measurement of air flow with variable orifice type flowmeters in laboratory experiments revealed discrepancies that could not be explained as errors arising from faulty calibration, leaks in the system, or failure to reduce readings to standard conditions of temperature and pressure. They were found to arise because of the occurrence of rapid pulsations in the air flow. A theoretical analysis of the effect showed that these instruments indicate root mean square rather than average flow rates. The results of experiments designed to test the theory were in reasonable agreement with the predicted values. It was found that errors arising from the occurrence of pulsations could be minimized by insertion of a suitable smoothing device between the pump and flowmeter. For example, an orifice with a pressure drop of 40 cm. of water reduced the flowmeter error to 5% of the true flow rate.

Introduction

Measurements of air flow in laboratory experiments led to inconsistencies depending on the point in a circuit at which flowmeters were inserted. The discrepancies could not be explained as due to errors in calibration of the flowmeter, leaks in the system, or failure to reduce readings to standard conditions of temperature and pressure.

Consideration of the principles underlying the operation of most types of flowmeters suggested a likely theoretical explanation in terms of a periodic variation in the flow rate. A simple metering layout was set up to demonstrate this phenomenon and the conditions under which it occurs. The arrangement was not felt to be entirely adequate for a test of the theory since there was considerable uncertainty as to the precise form and magnitude of pulsations in the air stream. A second experiment was designed specifically to test the theory.

Theory

A common feature noted in cases where flowmeters were giving readings not in harmony with other measurements was that in each case the meter was positioned where it might be subject to a pulsating flow rate. Consideration of the operating principles of most flowmeters reveals that the position of the indicating device is determined by fluid pressure. Only in a few special types are volume displacements or velocities measured directly. In the case of a rapidly varying flow rate the indicating device in most meters will take up a position corresponding to the average pressure encountered rather than the average velocity.

The theory that follows is for a tapered tube and float type of flowmeter, but it will apply with minor modification to all flowmeters which depend

[1] *Manuscript received February 20, 1950.*
Contribution from Defence Research Board, Experimental Station, Suffield, Alberta.
[2] *Seconded from Meteorological Service of Canada.*

for their metering action on the pressure gradient produced in a moving stream.

Consider a float of cross-sectional area A riding inside a tapered tube with a variable annular clearance of area a. If we assume completely turbulent flow downstream of the annulus, a flow rate V and a fluid density ρ, then neglecting a^2 in comparison to A^2 and neglecting viscosity the instantaneous force F on the float is:

$$F = \frac{A}{2}\rho\left(\frac{V}{a}\right)^2. \tag{1}$$

While the conditions postulated are approximately met in metering air in our experimental setup, an efficiency coefficient C can be introduced as in engineering practice to allow for departure from ideal conditions, giving:

$$V = aC\sqrt{\frac{2F}{A\rho}}. \tag{2}$$

For equilibrium under steady flow conditions this force is equated to the effective weight of the float Wg (expressed in suitable units).

$$Wg = \frac{A\rho}{2C^2}\left(\frac{V}{a}\right)^2. \tag{3}$$

Now consider flow through the meter in the form of rhythmic pulses, the flow rate V_t being a periodic function of time t, with period T. The pulses are assumed to be of such a frequency that the float cannot follow the individual pulsations but occupies a more or less steady mean position. The impulse on the float over the period T is given by

$$\int_0^T F dt = \int_0^T \frac{A\rho}{2C^2}\left(\frac{V_t}{a}\right)^2 dt. \tag{4}$$

For equilibrium with rapidly pulsating flow

$$Wg = \frac{1}{T}\int_0^T \frac{A\rho}{2C^2}\left(\frac{V_t}{a_e}\right)^2 dt, \tag{5}$$

where a_e is the annulus area a at the position of equilibrium. In turn, the calibrated steady flow rate V_e for this float position is given by (3) as

$$V_e = a_e C\sqrt{\frac{2Wg}{A\rho}}. \tag{6}$$

Substituted for a_e in (5)

$$Wg = \frac{1}{T}\int_0^T Wg\left(\frac{V_t}{V_e}\right)^2 dt. \tag{7}$$

This relation holds strictly only if C and ρ are constant (or if variable, the mean value over the range of conditions is equivalent to that at steady flow

value of V_e). While this constancy of C and ρ is not strictly true, the effect of variability is small and cannot mask the main effects studied here. The apparent flow rate metered is therefore

$$V_e = \left(\frac{1}{T}\int_0^T V_t^2\, dt\right)^{1/2}, \tag{8}$$

while the true mean flow rate is given by

$$\overline{V_t} = \frac{1}{T}\int_0^T V_t\, dt, \tag{9}$$

which in general for pulsating flow will differ markedly from the value given by (8).

Demonstration of Pulsation Error

The apparatus is sketched in Fig. 1. Air was circulated by a rotary vane type pump at E. This had three vanes, a displacement of 22 cc. per cycle,

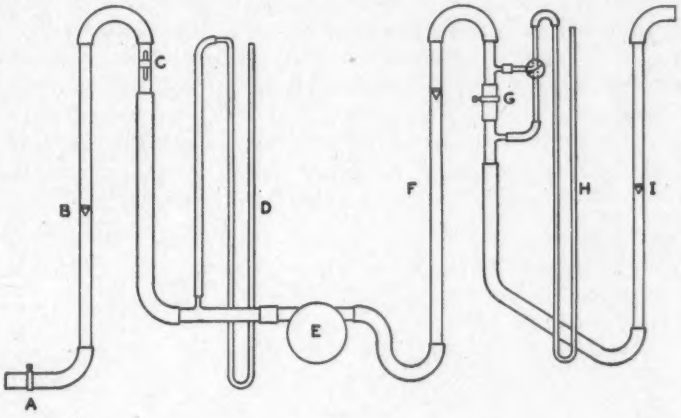

FIG. 1.

and rotated at 1760 r.p.m. The over-all flow rate was largely controlled by critical orifices inserted at C (i.e., an orifice running at sonic velocity and possessing constant flow-rate characteristics.) Flowmeters were placed at B, F, and I. These were of the tapered tube and float type and the calibration was checked by measured steady flow of air from a large aspirator bottle. Mercury manometers at D and H (the latter connected by a two way stop-cock) made it possible to determine pressure throughout the system. Further adjustments were made by means of clamps at A and G. The components were connected by glass and rubber tubing of internal diameter one-half inch or greater.

A critical orifice to regulate flow to a convenient rate was inserted at *C* and the pump turned on. The clamp at *A* was closed as a check for leaks in the system and the meter readings noted.

The clamp at *A* was opened, permitting circulation of air, and the flowmeters and manometers read. Clamp *G* was then gradually closed and a series of flowmeter and manometer readings obtained. Closing clamp *G* appeared to give rise to two effects. It smoothed the flow beyond and so caused flowmeter *I* to approach the true flow given by flowmeter *B*. It also lead to an initial rise in readings of flowmeter *F*, apparently by increasing the sharpness of the peaks delivered by the pump. The latter effect is obscure and was one reason for designing the more fundamental experiment described later. The degree of closing of this clamp was indicated by the rise in pressure between the pump and this point (Table I, "Pressure at outlet of F").

This procedure was repeated with two other critical orifices at *C*, giving a range of flow rates. The whole procedure was further repeated twice after interchanging flowmeters as a check on their calibration.

The results of the above experiment are given in Table I. For brevity, the observations with flowmeters interchanged are not given, as no change was apparent. The corrected flowmeter readings are reduced to volume flow at atmospheric pressure and room temperature. The temperature correction is a little uncertain. The temperature of the air leaving the pump (after running some time) was 325° A. but the air cooled rapidly to room temperature (290° A.) by the time it left flowmeter *F*. There should be no great error in taking

TABLE I

TEST COMPARISON OF FLOWMETERS

Run	Critical orifice	Flowmeter readings, liters/min.			Pressure, cm. of Hg				Corrected flowmeter readings			Ratio of reading flowmeter *F* to *B*
		B	*F*	*I*	Atmospheric	Between orifice and pump	At outlet of *F*	At inlet of *I*	*B*	*F*	*I*	
1	1	22.7	33.5	26.7	70.0	50.9	70.2	70.2	22.7	32.0	26.8	1.41
2		22.5	36.0	23.7	70.0	50.9	71.8	70.3	22.5	35.0	23.8	1.55
3		22.3	38.0	23.2	70.0	51.0	74.8	70.3	22.3	37.6	23.3	1.68
4		22.0	39.0	22.7	70.0	51.0	79.2	70.2	22.0	39.3	22.8	1.79
5	2	8.9	11.6	13.9	70.0	26.0	70.1	70.1	8.9	11.8	13.9	1.32
6		8.9	15.0	9.9	70.0	26.0	71.0	70.1	8.9	15.3	9.9	1.72
7		8.9	16.5	9.3	70.0	26.0	72.2	70.1	8.9	16.8	9.3	1.89
8		8.9	17.0	9.1	70.0	26.4	74.3	70.1	8.9	17.6	9.1	1.98
9		8.9	17.5	8.8	70.0	27.2	80.2	70.2	8.9	18.8	8.8	2.12
17	3	3.5	6.5	5.5	70.0	16.5	70.2	70.0	3.6	6.3	5.4	1.75
18		3.5	8.5	3.8	70.0	16.5	72.0	70.0	3.6	8.4	3.6	2.33
19		3.5	8.5	3.8	70.0	16.5	73.3	70.1	3.6	8.5	3.6	2.36
20		3.6	7.5	3.6	70.0	16.5	77.2	70.1	3.7	7.7	3.6	2.08

the air temperature for F as the mean (308° A.), since this will result in a total temperature correction of only 3% compared to that for the other flowmeters. The calibration corrections for the flowmeters were taken into account.

In all cases no leakage was indicated, the flowmeter at I showing no flow with clamp A closed. The float of the flowmeter at F rose slightly (below the bottom of the scale), but this can be expected with no net flow on the theory developed.

The simple theory of flowmeters normally used would lead one to expect the flowmeter readings at B, F, and I, given in Table I, to be identical. Another possible source of error is the effect of varying degrees of turbulence in the flow pattern through the meter. This could result in the meter at F reading slightly high but the error induced would be trivial beside the error observed

The theory derived earlier can be applied to the experimental data. In general, it is noticed that flowmeter F which received a sharply pulsating flow, read much higher than flowmeter B. The latter should be subject to practically steady flow because of the critical orifice. Changes in the experimental conditions which tended to increase the sharpness of the pulses from the pump also increased the positive departures of the readings given by F. Conversely, closing the clamp G so as to smooth out the pulses before reaching flowmeter I caused a reduction of the high reading of this flowmeter, so that it approached the value given by the steady flow at B.

Experimental Verification of Theory

An arrangement was devised whereby pulses of known form and amplitude might be superimposed on a controlled steady flow. The apparatus is sketched in Fig. 2.

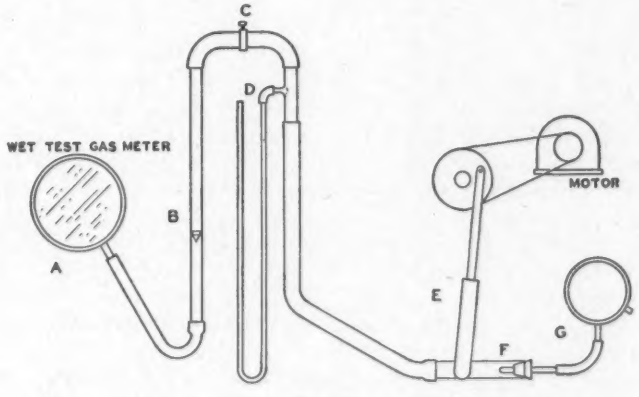

FIG. 2.

Air entering was metered by a Wet Test Gas Meter at A. The air then passed through a tapered tube and float flowmeter at B, through a critical orifice at F and a pump at G. At E a side connection led to a device for producing pulsations. This was a cylinder and piston, without valves, the piston being given a sinusoidal motion through a connecting rod and face plate turned at a controlled rate by a variable speed electric motor. During certain stages of the experiment, a clamp was placed on the line at C and a manometer inserted at D.

A critical orifice with a flow rate of approximately 10 liters per minute was inserted at F and the pump turned on. Steady flow rates were determined both on the flowmeter at B and by taking the flow through A over a half minute interval. The motor running the pulsating piston was then turned on and the speed regulated to a steady value. The speed was determined by observing the reciprocating parts with a mechanical stroboscope. The calibration for the latter had previously been checked (at both ends of the scale) against a tuning fork and a fluorescent light running at the power line frequency. Repeated measurements of flow rates were obtained both from the Wet Test Gas Meter and from the tapered tube flowmeter at various pulse speeds. The flow rates (at room temperature and pressure) and speeds of oscillation are given in Table II.

TABLE II

FLOW RATES FOR PULSED FLOW

Run	Pulsation rate, cycles/sec.	Wet Test Meter, liters/min.	Tapered tube meter, liters/min.	Theoretical root mean square flow, liters/min.
27	0	10.9	11.3	11.3
52	0	11.0	11.4	11.4
39	10.4	10.7	19.4	22.2
30	11.3	10.5	21.4	23.5
34	12.8	11.4	24.2	26.0
37	13.1	10.8	23.6	26.6
28	13.6	11.0	23.2	27.4
31	14.1	11.0	23.5	28.2
43	14.2	11.0	23.4	28.3
35	14.4	10.7	24.2	28.6
51	14.7	10.8	24.4	29.2
38	14.9	10.8	25.7	29.5
47	15.1	10.8	24.4	29.9
32	17.1	11.0	26.2	31.3
33	19.8	11.0	27.8	38.0

The diameter and travel of piston were measured and the piston displacement calculated. If A is the steady flow rate in cubic centimeters per second, D the displacement per piston stroke (13.7 cc.), and n, the number of cycles per second, then Q, the volume of air passing the meter in time t, will be given by

$$Q = At + \frac{D}{2} \sin 2\pi nt,$$

taking the initial time as that for which the phase angle is zero. The flow rate is given by

$$V_t = \frac{dQ}{dt} = A + \pi n D \cos 2\pi nt.$$

Substitution of the pulsation rate from Table II in this expression and use of Equation (8) give the flow rate that might be expected, on the theory developed here, to be indicated by any pressure operated meter. These figures are entered in the last column of Table II.

The constancy of the Wet Test Meter readings and the general agreement between the last two columns support the explanation given here for this phenomenon. The failure to obtain even closer agreement might be attributed to the damping of the pulse, compressibility and viscosity of the gas, and elasticity of the system. The effect of elasticity and capacity of the system was checked by doing two series of runs, in the first reducing connections between flowmeter and pulse source to a minimum and in the second adding a large additional path length. With connections consisting of 20 in. of 5/8 in. glass tubing, typical runs with no pulsation gave a meter reading of 11.3 liters per min. while an impressed pulsation rate of 14.6 cycles per sec. increased the flowmeter reading to 24.4 liters per min. Addition of 140 in. of 1/2 in. rubber tubing between flowmeter and pulse source gave a flow rate of 11.1 liters per min. for steady flow and a meter reading of 24.1 liters per min. for a pulsation rate of 14.4 cycles per sec. It is thus apparent that pulse damping in the system is not an adequate explanation of the remaining discrepancy. Another factor which may be of importance is the failure of the float to ride in its normal stable attitude when supported by a pulsating stream, with consequent change in the efficiency coefficient C. Evidence to support this view was provided by mounting a flowmeter on a vibrating stand. With the stand steady and flow controlled by a critical orifice, a flowrate of 10.7 liters per sec. was recorded, while with the stand vibrating (amplitude of the order of 1 mm. and frequency 60 cycles per sec.) the indicated flow fell to 9.7 liters per sec.

It might be argued that the constancy of flow rate indicated by the Wet Test Meter did not necessarily indicate that this meter gave true average flow rates independent of any pulsations, since the tapered tube meter might have absorbed all the pulsations. Two tapered tube meters were therefore inserted in series. A series of runs at various pulse rates showed no difference in indicated flow rate between the two meters. It can be concluded that a single tapered tube flowmeter has no appreciable smoothing effect on pulse form.

Application

In line with the earlier discussion it was felt desirable to find just what pressure drop was necessary to reduce to a reasonable figure the error introduced by pulsation. The apparatus was assembled as in Fig. 2 with an adjust-

able clamp at *C* and a manometer at *D*. A series of runs were made with the clamp *C* first set for open flow and then adjusted to reduce the error to 50% and to 5% of the true flow. Typical results are given in Table III.

TABLE III

PULSE SMOOTHING THROUGH A CONSTRICTION

Run	Pulsation rate, cycles/sec.	Pressure drop at constriction, cm. of water	Wet Test Meter, liters/min.	Tapered tube meter, liters/min.
44	0	0	11.0	11.4
51	14.7	0	10.8	24.5
45	0	5.5	11.0	11.3
46	14.7	13	10.5	17.6
49	0	34	10.2	10.5
50	16.0	39	10.2	11.1

The flowmeter errors with unrestricted pulsing flow in these cases are similar to those found earlier for an ordinary laboratory rotary vane pump. It is apparent that to reduce flow metering error to 5% or less in circuits including the usual laboratory pumps, careful thought must be given to inserting an adequate smoothing device between pump and meter. An orifice running at critical velocity is suitable, but, with subcritical orifices, a maximum velocity in the neighborhood of 100 meters a second must be reached to provide the necessary pressure drop of 40 cm. of water. Provision of considerable reservoir capacity between orifice and pump might reduce to some extent the pressure fall required through the orifice.

Conclusions

The true average flow rate is not given by variable orifice type flowmeters when used to measure rapidly pulsating flow. This circumstance is due to the fact that most flowmeters measure pressures and forces, and so the mean reading is the root mean square flow rather than the arithmetic mean. The only notable exceptions are flowmeters which measure by volume displacement.

Owing to the nature of the flow from most forms of circulating pumps, this error can be serious in experimental work. Measurement of flow rate in systems using ordinary laboratory pumps requires the placing of some device between pump and meter to reduce the "ripple" in flow rate to a moderate figure. Fortunately, the error decreases rapidly with smoothing of pulse form. Either a critical orifice or carefully chosen subcritical orifice and expansion chamber should suffice.